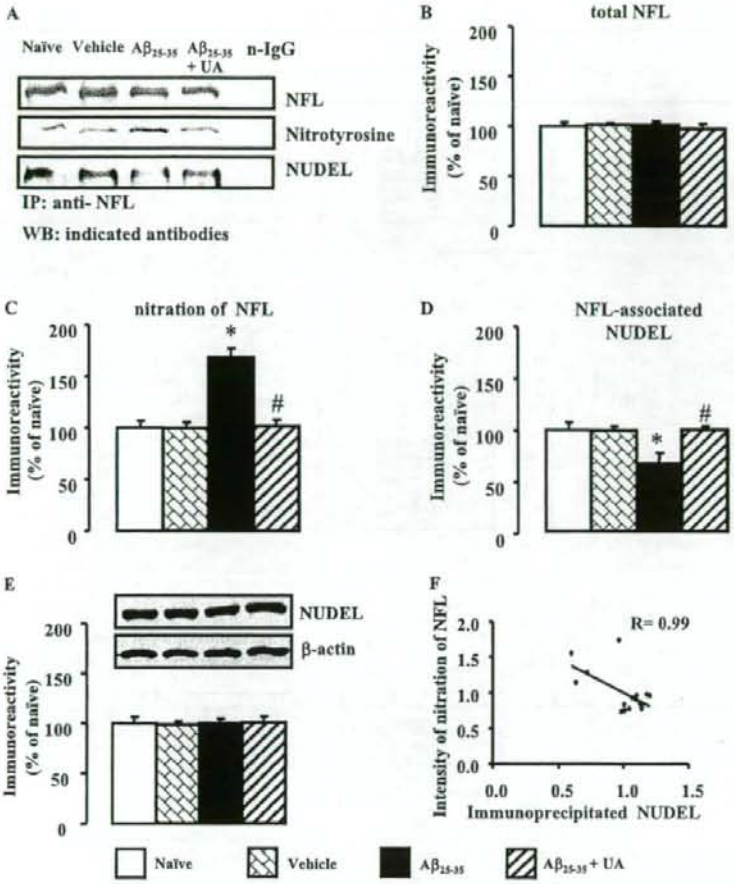

Fig. 5. Association between the extensive nitration of NFL and the reduced interaction with NUDEL in the Triton X-100-soluble fraction. A, the immunocomplexes obtained with the anti-NFL antibody, from precleared protein samples of the hippocampal homogenates, were separated by SDS-PAGE, blotted onto a PVDF membrane, and probed with the indicated antibodies. B, equal amounts of NFL protein were obtained. C, tyrosine nitration of NFL was increased in the $A\beta_{25-35}$ group, whereas UA treatment prevented the increase. D, the level of NFL-interacting NUDEL was reduced in the $A\beta_{25-35}$ group, whereas UA treatment prevented the reduction. E, no difference in NUDEL protein expression was found among the groups. F, the increased nitration of NFL was associated with reduced interaction with NUDEL. The intensity of bands was quantified and expressed as a percentage of that in the naive group. Data were presented as the mean ± S.E. ($n = 4$). *, $p < 0.05$ versus naive and vehicle; #, $p < 0.05$ versus $A\beta_{25-35}$.

Sultana et al., 2006), the proteomic detections on various conditions (Castegna et al., 2003; Sultana et al., 2006), immunodetections by means of different anti-nitrotyrosine antibodies with the diverse recognition property for nitrotyrosine (Strong et al., 1998; Tran et al., 2003), or the biological selectivity of tyrosine nitration (Ischiropoulos, 2003; Sacksteder et al., 2006). Dissimilar reports about the nitrated proteins in the brains of humans with Alzheimer's disease (AD) (Castegna et al., 2003; Sultana et al., 2006) emphasize the importance of the sources of protein, even in the same species or under the same conditions of detection during the identification process, while illustrating the diversity of nitration due to the dissimilar expression of proteins during the different stages of the disease.

In the present study, we looked for further evidence for the pathogenic role of protein nitration as one of the key contributors to the decline of cognitive function induced by Aβ. Using LC-MS/MS and immunodetection, we identified the hippocampal proteins with nitrated tyrosine residues after the i.c.v. injection of $A\beta_{25-35}$ in mice. Preferentially, in respect with currently examined proteins, intense nitration of NFL was observed, demonstrating a good correlation with the severity of cognitive impairment induced by $A\beta_{25-35}$.

NFL, one of the three subunits of NF proteins, is the indispensable core of the NF assembly (Zhu et al., 1997). Studies have reported that NFL is selectively nitrated compared with the majority of other proteins present in brain homogenates, and they suggested that newly synthesized free NFL is particularly susceptible to peroxynitrite-mediated nitration (Crow et al., 1997; Strong et al., 1998). The extensively nitrated NFL inhibits the assembly of unmodified NF subunits (Crow et al., 1997). On the other hand, the extensive serine phosphorylation of NFL could sufficiently block NF assembly (Nixon and Shea, 1992; Gibb et al., 1996). Therefore, we have evaluated the effect of tyrosine nitration on the phosphorylation of NFL at serine residues in general. The increased tyrosine nitration of NFL was associated with its serine hyperphosphorylation. Prevention of the extensive nitration of NFL by UA, a scavenger of $ONOO^-$ that nitrates proteins, restrained the serine phosphorylation of NFL at a normal level. The results indicated that the increased nitration of NFL could give rise to its serine hyperphosphorylation.

NFL requires direct binding with NUDEL, whereas NUDEL can not directly bind with other subunits of NF proteins, to initiate the assembly of NF (Nguyen et al., 2004). After the assembly of the NF network, NUDEL remains bound to the assembled Triton X-100-insoluble neurofilaments and may promote, in conjunction with molecular mo-

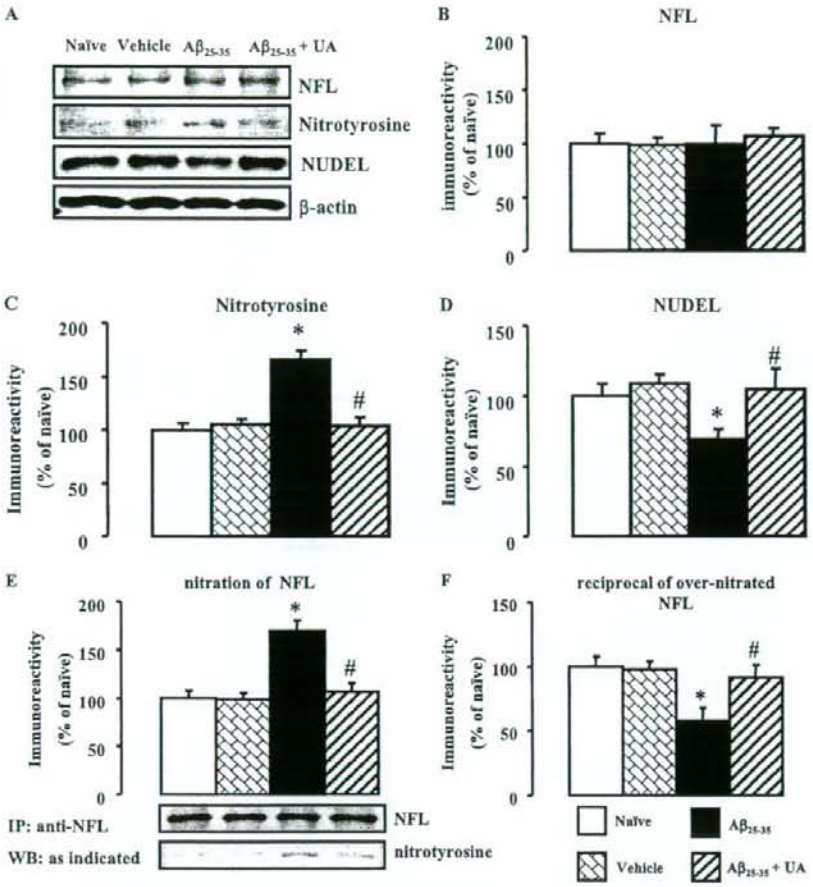

Fig. 6. The reduced content of NUDEL in the Triton X-100-insoluble cytoskeletal fraction. The Triton X-100-insoluble fraction, including cytoskeletal proteins, was solubilized in 6 M urea. A, equal amounts of protein were subjected to Western blot analysis. B, the protein levels of NFL were unchanged in all groups. C, the intensity of nitrotyrosine was increased in the $A\beta_{25-35}$ group, and the increase was prevented by UA, a scavenger of $ONOO^-$ that nitrates tyrosine. D, the protein level of NUDEL was reduced in the $A\beta_{25-35}$ group, and UA prevented this reduction. The quantified intensity of the bands was corrected by that of β-actin and expressed as a percentage of that in the naive group. E, equal amounts of NFL protein were immunoprecipitated and probed with anti-nitrotyrosine antibodies. The intensity of nitrotyrosine in NFL was increased in the $A\beta_{25-35}$ group, whereas UA prevented any increase. F, the reciprocal of the overnitrated NFL was estimated by applying multiplicative inverse (or reciprocal, in which the reciprocal of n is 1/n). The intensity of bands was quantified and expressed as a percentage of that in the naive group. Data are presented as the mean ± S.E. ($n = 4$). *, $p < 0.05$ versus naive and vehicle; #, $p < 0.05$ versus $A\beta_{25-35}$.

tors, the axonal transport of the neurofilaments (Nguyen et al., 2004). Thus, the level of interaction between NFL and NUDEL in the Triton X-100-soluble cytoplasmic fraction could be reflected by their protein levels in the Triton X-100-insoluble cytoskeletal fraction. In the current study, the increased nitration of Triton X-100-soluble NFL proteins in the $A\beta_{25-35}$ group was associated with its decreased interaction with NUDEL. In the Triton X-100-insoluble fraction, the protein level of NUDEL was reduced in the $A\beta_{25-35}$ group, and the reduction was prevented by treatment with UA. In the same fraction, the protein level of NFL surprisingly did not differ among groups, whereas the intensity of the nitration of NFL was strong in $A\beta_{25-35}$ group. Estimation by the multiplicative inverse approach indicated that the reduced level of nonextensively nitrated NFL in the $A\beta_{25-35}$ group parallels with that of NUDEL. These results required an explanation for the detection of the extensively nitrated NFL in the Triton X-100-insoluble cytoskeletal fraction, because the assembled NFL is nitration-resistant and the intensely nitrated NFL can not participate in the NF assembly (Crow et al., 1997). The alteration of the solubility of the overnitrated NFL might be involved in the detection of the extensively nitrated NFL in the Triton X-100-insoluble cytoskeletal fraction in the $A\beta_{25-35}$ group. Interpretation of the emergence of the intensely nitrated NFL in PBS-insoluble, but Triton X-100-soluble, protein pools in the $A\beta_{25-35}$ group indicates that extensive nitration would render NFL protein to have poor solubility in PBS. By this rate, it is possible that a considerable level of overnitrated NFL protein in the $A\beta_{25-35}$ group would even become Triton X-100 insoluble over a period of time, and that it would be detected along with a reduced level of NUDEL-associated assembled NFL, which is also Triton X-100 insoluble. The observation of detectable levels of nitration in NFL in the RIPA-soluble, Triton X-100-soluble, and Triton X-100-insoluble fractions in the naive and vehicle groups implies that natural nitration of tyrosine, as serine phosphorylation, might exist as a physiological property of NFL and might not be detrimental to the function of the protein, whereas extensive nitration is detrimental. The nitration-susceptible tyrosine residues of NFL are identified particularly as tyrosine 17 in the head region and tyrosines 138, 177, and 265 in the α-helical coil regions of the rod domain of the protein (Crow et al., 1997). It needs to be determined which tyrosine residue is the site for natural nitration or for extensive nitration. It has been reported that, although the exact mechanism is not clear, the newly synthesized Triton X-100-soluble NF proteins, including NFL, could separately undergo axonal transport before being in-

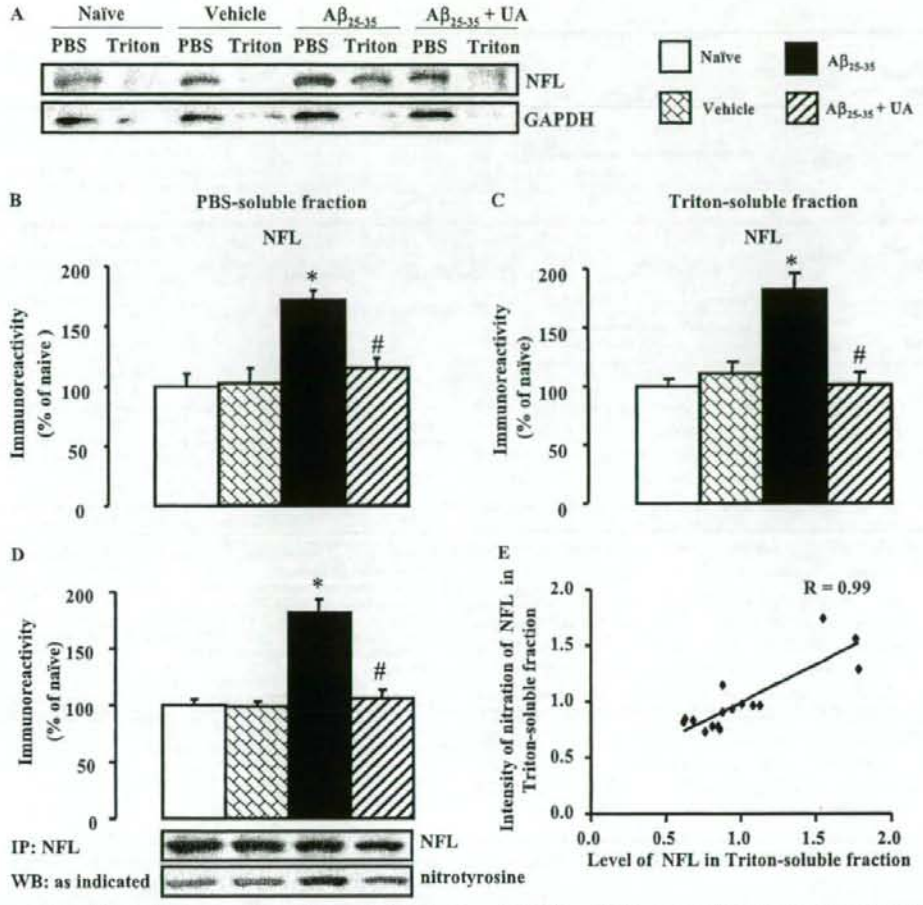

Fig. 7. The association of the extensive nitration of NFL with the alteration of solubility. The hippocampal tissues were homogenated in PBS and centrifuged at 13000*g* for 20 min, the washed pellets were solubilized in Triton X-100 as described under *Materials and Methods*, and equal amounts of protein were subjected to Western blot analysis. A to C, a majority of NFL and GAPDH proteins were soluble in PBS. NFL protein in the $A\beta_{25-35}$ group in both the PBS-soluble fraction and the Triton X-100-soluble fraction was increased, and the increase was prevented by UA, a scavenger of $ONOO^-$ that nitrates tyrosine. The quantified intensity of the bands was corrected by that of GAPDH and expressed as a percentage of that in the naive group. D, equal amounts of NFL from the Triton X-100-soluble proteins were immunoprecipitated and probed with anti-nitrotyrosine antibodies. The intensity of nitrotyrosine in NFL was increased in the $A\beta_{25-35}$ group, whereas UA prevented the increase. The intensity of bands was quantified and expressed as a percentage of that in the naive group. E, the level of NFL in the Triton X-100-soluble (PBS-insoluble) fraction was associated with the intensity of its nitration. Data are presented as the mean ± S.E. (n = 4). *, $p < 0.05$ versus naive and vehicle; #, $p < 0.05$ versus $A\beta_{25-35}$.

TABLE 2
The Nissl-positive cells in the hippocampus
In each group, n = 4.

Subfields of Hippocampus	Number of Nissl-Positive Cells			
	Naive	Vehicle	$A\beta_{25-35}$	$A\beta_{25-35}$ + UA
	counts/mm²			
CA1	10800 ± 230	10900 ± 290	10850 ± 250	10790 ± 270
CA3	6750 ± 190	6690 ± 210	6698 ± 180	6680 ± 310
GrDG	21000 ± 670	20980 ± 590	20990 ± 710	20780 ± 690

GrDG, the granular layer of the dentate gyrus.

corporated into the Triton X-100-insoluble axonal cytoskeleton (Jung et al., 1998). We do not know whether the NFL proteins with natural nitration undergo axonal transport after the NF assembly or undergo axonal transport before being incorporated into the Triton X-100-insoluble axonal cytoskeleton.

The observation of no cell loss in CA1, CA3, and the granular layer of the dentate gyrus of the hippocampus in mice

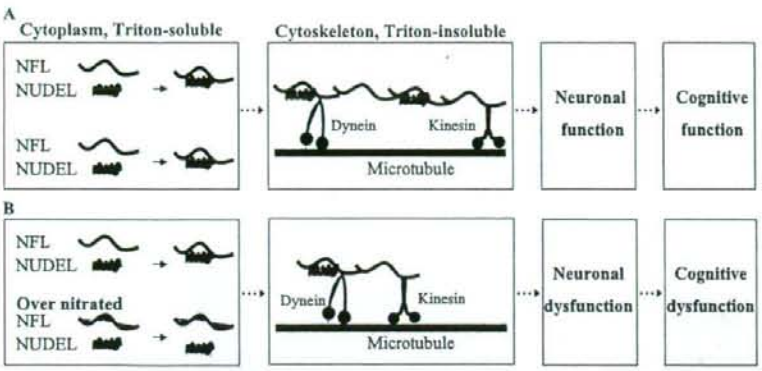

Fig. 8. The contribution of the extensive nitration of NFL to cognitive dysfunction. A, in this model, NFL interacts with NUDEL, which is essential for the incorporation of NF subunits into the network during NF assembly and elongation. A normal NF assembly and elongation favors normal neuronal and cognitive functions. B, the overnitration of NFL disrupts the interaction of NFL with NUDEL and may lead to the defective assembly of NF and abnormalities in neuronal and cognitive functions. The resized microtubules, kinesin, and dyenin have been added for clarity (modified from Nguyen et al., 2004; Holzbaur, 2004).

that received $A\beta_{25-35}$ injections favored the contribution of extensive nitration of NFL to the impairment of memory. A recent study demonstrated that rapidly formed fresh amyloid plaques cause axonal and dendritic structural changes within a minimum of 5 days after the "birth of the plaques" (Meyer-Luehmann et al., 2008). Given the time windows of Aβ neurotoxicity, $A\beta_{25-35}$ may require longer time to cause cell loss in our mouse model of cognitive impairment.

The disrupted interaction between NFL and NUDEL is regarded as the most important factor for the destabilization of the NF assembly that leads to the axonal dysfunction, which is an early event in the cognitive pathology of AD (Nguyen et al., 2004; Stokin et al., 2005). Therefore, our results suggest that disrupted interaction between NUDEL and NFL with extensive nitration could be one of the major factors that associated with the cognitive dysfunction induced by Aβ in mice (Fig. 8). However, further studies are required to investigate whether the extensive nitration of NFL and the impaired interaction with NUDEL induced by Aβ are associated with the disruption of axonal transport.

Acknowledgments

We are grateful to Dr. Minh Dang Nguyen for discussions on the sample preparation.

References

Alkam T, Nitta A, Mizoguchi H, Itoh A, and Nabeshima T (2007) A natural scavenger of peroxynitrites, rosmarinic acid, protects against impairment of memory induced by Aβ25–35. *Behav Brain Res* **180**:139–145.

Alkam T, Nitta A, Mizoguchi H, Saito K, Seshima M, Itoh A, Yamada K, and Nabeshima T (2008) Restraining tumor necrosis factor-alpha by thalidomide prevents the amyloid beta-induced impairment of recognition memory in mice. *Behav Brain Res* **189**:100–106.

Andersen JK (2004) Oxidative stress in neurodegeneration: cause or consequence? *Nat Med* **10**:S18–S25.

Aoyama Y and Kitajima Y (1999) Pemphigus vulgaris-IgG causes a rapid depletion of desmoglein 3 (Dsg3) from the Triton X-100 soluble pools, leading to the formation of Dsg3-depleted desmosomes in a human squamous carcinoma cell line, DJM-1 cells. *J Invest Dermatol* **112**:67–71.

Bastianetto S and Quirion R (2004) Natural antioxidants and neurodegenerative diseases. *Front Biosci* **9**:3447–3452.

Black MM, Keyser P, and Sobel E (1986) Interval between the synthesis and assembly of cytoskeletal proteins in cultured neurons. *J Neurosci* **6**:1004–1012.

Castegna A, Thongboonkerd V, Klein JB, Lynn B, Markesberyl WR, and Butterfield DA (2003) Proteomic identification of nitrated proteins in Alzheimer's disease brain. *J Neurochem* **85**:1394–1401.

Crow JP, Ye YZ, Strong M, Kirk M, Barnes S, and Beckman JS (1997) Superoxide dismutase catalyzes nitration of tyrosines by peroxynitrite in the rod and head domains of neurofilament-L. *J Neurochem* **69**:1945–1953.

Dalle-Donne A, Scaloni D, Giustarini E, Cavarra G, Tell G, Lungarella R, Colombo R, Rossi R, and Milzani A (2005) Proteins as biomarkers of oxidative/nitrosative stress in diseases: the contribution of redox proteomics. *Mass Spectrom Rev* **24**: 55–99.

Gibb BJ, Robertson J, and Miller CC (1996) Assembly properties of neurofilament light chain Ser55 mutants in transfected mammalian cells. *J Neurochem* **66**:1306–1311.

Hisanaga S, Gonda Y, Inagaki M, Ikai A, and Hirokawa N (1990) Effects of phosphorylation of the neurofilament L protein on filamentous structures. *Cell Regul* **1**:237–248.

Holzbaur EL (2004) Tangled NUDELs? *Nat Cell Biol* **6**:569–570.

Ischiropoulos H (2003) Biological selectivity and functional aspects of protein tyrosine nitration. *Biochem Biophys Res Commun* **305**:776–783.

Jung C, Yabe J, Wang FS, and Shea TB (1998) Neurofilament subunits can undergo axonal transport without incorporation into Triton-insoluble structures. *Cell Motil Cytoskeleton* **40**:44–58.

Keller JN (2006) Oxidative damage and oxidative stress in Alzheimer's disease. *Res Pract Alzheimer's Dis* **11**:110–114.

Kim HC, Yamada K, Nitta A, Olariu A, Tran MH, Mizuno M, Nakajima A, Nagai T, Kamei H, Jhoo WK, et al. (2003) Immunocytochemical evidence that amyloid beta (1–42) impairs endogenous antioxidant systems in vivo. *Neuroscience* **119**:399–419.

Koppal T, Drake J, Yatin S, Jordan B, Varadarajan S, Bettenhausen L, and Butterfield DA (1999) Peroxynitrite-induced alterations in synaptosomal membrane proteins: insight into oxidative stress in Alzheimer's disease. *J Neurochem* **72**:310–317.

Kubo T, Nishimura S, Kumagae Y, and Kaneko I (2002) In vivo conversion of racemized beta-amyloid ([D-Ser 26]A beta 1–40) to truncated and toxic fragments ([D-Ser 26]A beta 25–35/40) and fragment presence in the brains of Alzheimer's patients. *J Neurosci Res* **70**:474–483.

Lim GP, Chu T, Yang F, Beech W, Frautschy SA, and Cole GM (2001) The curry spice curcumin reduces oxidative damage and amyloid pathology in an Alzheimer transgenic mouse. *J Neurosci* **21**:8370–8377.

Maurice T, Lockhart BP, and Privat A (1996) Amnesia induced in mice by centrally administered beta-amyloid peptides involves cholinergic dysfunction. *Brain Res* **706**:181–193.

Meyer-Luehmann M, Spires-Jones TL, Prada C, Garcia-Alloza M, de Calignon A, Rozkalne A, Koenigsknecht-Talboo J, Holtzman DM, Bacskai BJ, and Hyman BT (2008) Rapid appearance and local toxicity of amyloid-beta plaques in a mouse model of Alzheimer's disease. *Nature* **451**:720–724.

Nabeshima T, Katoh A, Ishimaru H, Yoneda Y, Ogita K, Murase K, Ohtsuka H, Inari K, Fukuta T, and Kameyama T (1991) Carbon monoxide-induced delayed amnesia, delayed neuronal death and change in acetylcholine concentration in mice. *J Pharmacol Exp Ther* **256**:378–384.

Nguyen MD, Shu T, Sanada K, Larivière RC, Tseng HC, Park SK, Julien JP, and Tsai LH (2004) A NUDEL-dependent mechanism of neurofilament assembly regulates the integrity of CNS neurons. *Nat Cell Biol* **6**:595–608.

Nitta A, Fukuta T, Hasegawa T, and Nabeshima T (1997) Continuous infusion of beta-amyloid protein into the rat cerebral ventricle induces learning impairment and neuronal and morphological degeneration. *Jpn J Pharmacol* **73**:51–57.

Nixon RA and Shea TB (1992) Dynamics of neuronal intermediate filaments: a developmental perspective. *Cell Motil Cytoskeleton* **22**:81–91.

Perry G, Nunomura A, Hirai K, Zhu X, Pérez M, Avila J, Castellani RJ, Atwood CS, Aliev G, Sayre LM, et al. (2002) Is oxidative damage the fundamental pathogenic mechanism of Alzheimer's and other neurodegenerative diseases? *Free Rad Biol Med* **33**:1475–1479.

Pike CJ, Walencewicz-Wasserman AJ, Kosmoski J, Cribbs DH, Glabe CG, and Cotman CW (1995) Structure-activity analyses of Aβ peptides: contributions of the β25–35 region to aggregation and neurotoxicity. *J Neurochem* **64**:253–265.

Reynolds MR, Berry RW, and Binder LI (2007) Nitration in neurodegeneration: deciphering the "Hows" "nYs". *Biochemistry* **46**:7325–7336.

Sacksteder CA, Qian WJ, Knyushko TV, Wang H, Chin MH, Lacan G, Melega WP, Camp DG 2nd, Smith RD, Smith DJ, et al. (2006) Endogenously nitrated proteins in mouse brain: links to neurodegenerative disease. *Biochemistry* **45**:8009–8022.

Sano M, Ernesto C, Thomas RG, Klauber MR, Schafer K, Grundman M, Woodbury P, Growdon J, Cotman CW, Pfeiffer E, et al. (1997) A controlled trial of selegiline, alpha-tocopherol, or both as treatment for Alzheimer's disease. The Alzheimer's Disease Cooperative Study. *N Engl J Med* **336**:1216–1222.

Silberberg JS (1990) Estimating the benefits of cholesterol lowering: are risk factors for coronary heart disease multiplicative? *J Clin Epidemiol* **43**:875–879.

Smith MA, Richey Harris PL, Sayre LM, Beckman JS, and Perry G (1997) Wide-

spread peroxynitrite-mediated damage in Alzheimer's disease. *J Neurosci* **17**: 2653–2657.
Stokin GB, Lillo C, Falzone TL, Brusch RG, Rockenstein E, Mount SL, Raman R, Davies P, Masliah E, Williams DS, et al. (2005) Axonopathy and transport deficits early in the pathogenesis of Alzheimer's diseases. *Science* **307**:1282–1288.
Strong MJ, Sopper MM, Crow JP, Strong WL, and Beckman JS (1998) Nitration of the low molecular weight neurofilament is equivalent in sporadic amyotrophic lateral sclerosis and control cervical spinal cord. *Biochem Biophys Res Commun* **248**:157–164.
Sultana R, Poon HF, Cai J, Pierce WM, Merchant M, Klein JB, Markesbery WR, and Butterfield DA (2006) Identification of nitrated proteins in Alzheimer's disease brain using a redox proteomics approach. *Neurobiol Dis* **22**:76–87.
Tohda C, Tamura T, and Komatsu K (2003) Repair of amyloid beta (25–35)-induced memory impairment and synaptic loss by a Kampo formula, Zokumei-to. *Brain Res* **990**:141–147.
Tran MH, Yamada K, Nakajima A, Mizuno M, He J, Kamei H, and Nabeshima T (2003) Tyrosine nitration of a synaptic protein synaptophysin contributes to amyloid β-peptide-induced cholinergic dysfunction. *Mol Psychiatry* **8**:407–412.
Walsh DM and Selkoe DJ (2004) Deciphering the molecular basis of memory failure in Alzheimer's disease. *Neuron* **44**:181–193.
Yamada K, Tanaka T, Han D, Senzaki K, Kameyama T, and Nabeshima T (1999) Protective effects of idebenone and alpha-tocopherol on beta-amyloid-(1–42)-induced learning and memory deficits in rats: implication of oxidative stress in beta-amyloid-induced neurotoxicity in vivo. *Eur J Neurosci* **11**:83–90.
Zhu Q, Couillard-Després S, and Julien JP (1997) Delayed maturation of regenerating myelinated axons in mice lacking neurofilaments. *Exp Neurol* **148**:299–316.

Address correspondence to: Dr. Toshitaka Nabeshima, Department of Chemical Pharmacology, Graduate School of Pharmaceutical Science, Meijo University, Nagoya 468-8503, Japan. E-mail: tnabeshi@ccmfs.meijo-u.ac.jp

Molecular Psychiatry (2008) 13, 451–463

www.nature.com/mp

ORIGINAL ARTICLE

Identification of Piccolo as a regulator of behavioral plasticity and dopamine transporter internalization

X Cen[1,2], A Nitta[1], D Ibi[1,3], Y Zhao[1], M Niwa[1], K Taguchi[1], M Hamada[1], Y Ito[3], Y Ito[4], L Wang,[2] and T Nabeshima[1,5]

[1]Department of Neuropsychopharmacology and Hospital Pharmacy, Nagoya University Graduate School of Medicine, Nagoya, Japan; [2]National Chengdu Center for Safety Evaluation of Drugs, West China Hospital, Sichuan University, Chengdu, China; [3]Department of Pharmacology, College of Pharmacy, Nihon University, Chiba, Japan; [4]Equipment Center for Research and Education, Nagoya University Graduate School of Medicine, Nagoya, Japan and [5]Department of Chemical Pharmacology, Meijo University Graduate School of Pharmaceutical Sciences, Nagoya, Japan

Dopamine transporter (DAT) internalization is a mechanism underlying the decreased dopamine reuptake caused by addictive drugs like methamphetamine (METH). We found that Piccolo, a presynaptic scaffolding protein, was overexpressed in the nucleus accumbens (NAc) of the mice repeatedly administrated with METH. Piccolo downexpression by antisense technique augmented METH-induced behavioral sensitization, conditioned reward and synaptic dopamine accumulation in NAc. Expression of Piccolo C_2A domain attenuated METH-induced inhibition of dopamine uptake in PC12 cells expressing human DAT. Consistent with this, it slowed down the accelerated DAT internalization induced by METH, thus maintaining the presentation of plasmalemmal DAT. In immunostaining and structural modeling Piccolo C_2A domain displays an unusual feature of sequestering membrane phosphatidylinositol 4,5-bisphosphate, which may underlie its role in modulating DAT internalization. Together, our results indicate that Piccolo upregulation induced by METH represents a homeostatic response in the NAc to excessive dopaminergic transmission. Piccolo C_2A domain may act as a cytoskeletal regulator for plasmalemmal DAT internalization, which may underlie its contributions in behavioral plasticity.
Molecular Psychiatry (2008) **13**, 451–463; doi:10.1038/sj.mp.4002132; published online 15 January 2008

Keywords: Piccolo; dopamine transporter; methamphetamine; behavioral plasticity; C_2A domain

Introduction

Dopamine transporter (DAT), a member of the Na^+/Cl^--dependent transporters in the dopaminergic neurons, is critical for terminating dopamine (DA) neurotransmission and contributes to the abuse potential of psychostimulants. The stimulating and reinforcing effects of drugs result from enhanced synaptic DA accumulation in specific brain areas like nucleus accumbens (NAc). Cocaine and methamphetamine (METH; or its analogue amphetamine) elevate extracellular DA by inhibiting DA reuptake through DAT and, in the case of METH, also by promoting reverse transport of nonvesicular DA, reducing plasma membrane DAT through internalization, and displacing DA from synaptic vesicle (SV) to the cytoplasm.[1,2]

Membrane trafficking of DAT is closely associated with DA homeostasis and synaptic plasticity, and increasing evidences have showed that METH-like drugs are able to modulate this dynamic process.[3] The internalization of plasmalemmal DAT is a clathrin-mediated process,[4,5] and internalized DAT can be sorted to endosomal compartments where they may be recycled to cell surface and/or lysosome for degradation.[6] Inhibition of endocytic machinery assembly can attenuate amphetamine- or phorbol ester-mediated DAT internalization,[7] whereas expression of endosomal proteins like Rab5 in endosomal vesicles promotes amphetamine-induced intracellular DAT accumulation.[8] These findings strongly suggest that manipulation of endocytic components could be an important manner for regulating DAT internalization.

Piccolo, a component of the presynaptic cytoskeletal matrix, is assembled ultrastructurally as an electron-dense region of filaments at the active zone (AZ). It is proposed to play a scaffolding role in regulating AZ assembly,[9] actin cytoskeleton and SV trafficking.[10,11] Piccolo contains multiple subdomains including PDZ domain and Ca^{2+}/phospholipid binding (C_2A and C_2B) domains, each of which exhibits

Correspondence: Professor T Nabeshima, Department of Chemical Pharmacology, Meijo University Graduate School of Pharmaceutical Sciences, 150 Yagotoyama, Tenpaku, Nagoya 468-8503, Japan.
E-mail: tnabeshi@ccmfs.meijo-u.ac.jp
Received 17 June 2007; revised 14 September 2007; accepted 21 September 2007; published online 15 January 2008

distinctive features.[10,12] PDZ domain may interact with other presynaptic molecules involving molecule anchoring and assembly at AZ.[13] C_2A domain shows an unusual ability to sense intracellular changes of Ca^{2+} levels and then trigger the association with membrane phospholipids (PIs) via electrostatic interaction.[14] Notably, it interacts with phosphatidylinositol 4,5-bisphosphate (PIP_2),[15] a critical molecule for actin dynamics and endocytosis. It is well established that PIP_2 coordinates membrane fusion with actin filament to promote membrane movement, and recruits accessory adaptors for clathrin-coated pits.[16] Therefore, modulation of plasmalemmal PIP_2 may affect PIP_2-dependent biological processes like membrane trafficking and endocytosis.

In this study we find that Piccolo servers as a negative presynaptic modulator for behavioral hypersensitivity and blunts excessive dopaminergic synaptic plasticity by regulating plasmalemmal DAT internalization. Moreover, Piccolo C_2A domain may contribute to such distinct effects by targeting membrane PIP_2.

Materials and methods

Material

A pCMV-hDAT expression plasmid was kindly provided by Dr Marc Caron (Duke University Medical Center). The expression plasmids of pCMV-HA-Piccolo-PDZ (amino acid 3900–4244), pCMV-Myc-Piccolo-C_2A (amino acid 4704–5610) and pGEX4T-GST-p13192 (amino acid 4364–4755; named p13192) were constructed as previously described.[17] The following antibodies were used: hDAT and tyrosine hydroxylase (TH; Chemicon International Inc., Billerica, MA); hemagglutinin epitope (HA) and c-Myc (Cell Signaling, Billerica, MA); GST (Amersham Biosciences, Uppsala, Sweden); Piccolo and Rim 2 (Synaptic Systems, Albany, OR); PIP_2 (Assay Designs, Ann Arbor, MI, USA); syntaxin 1A (Santa Cruz Biotechnology, Santa Cruz, CA); synaptophysin (Sigma-Aldrich, St Louis, MO). The following reagents were used: botulinum neurotoxin (Bont)/C1 and Bont/B (Wako Pure Chemical Industries Ltd, Osaka, Japan); sulfo-NHS-biotin and immobilized streptavidin (Pierce, Rockford, IL).

RT–PCR and real-time RT–PCR

Isolation of total RNA from the NAc of mice was performed using RNeasy Mini Kit (QIAGEN, Hilden, Germany). The mRNA productions from nine target cDNA sequences of Piccolo were assayed by reverse transcription (RT)–PCR, followed by electrophoresis. The forward and reverse primers for the nine sequences were shown in Supplementary Table 1. Piccolo mRNA levels in brain NAc were validated by quantitative real-time RT–PCR using an iCycler System (Bio-Rad, Hercules, CA). Briefly, isolation of total RNA was performed using RNeasy Mini Kit (QIAGEN). For reverse transcription, 1 μg RNA was converted into a cDNA by a standard 20 μl reverse transcriptase reaction using oligo (dT) primers (Invitrogen, Hercules, CA) and Superscript II RT (Bio-Rad Laboratories, Hercules, CA, USA). Total cDNA (1 μl) was amplified in a 25 μl reaction mixture using 0.1 μM each of forward and reverse primers and Platinum Quantitative PCR SuperMix-UDG (Invitrogen). The primer and dye probes were designed by Nippon Gene Co. Ltd (Tokyo, Japan) using Primer Express software. The forward primer was 5′-GGATAGCGCACAAGGTTTTCC-3′ (base pair 4180–4200) with reverse being 5′-TTCAACCGAAT CATAGGATGCTC-3′ (base pair 4257–4279), and the dye probe was 5′-CACAAAGAGAATCCTGAGCTGG TCGATGA-3′ (base pair 4192–4220). Ribosomal mRNA was used and determined as control for RNA integrity with TaqMan ribosomal RNA control reagents.

Antisense

An antisense oligodeoxynucleotide (AS; 5′-CTCTGCC AAAACTTC-3′) and a scramble oligodeoxynucleotide (SC; 5′-AACGTAGTCACGTAG-3′) were synthesized by Nippon Gene Co. Ltd. C57BL/6 mice were infused intracerebroventricularly with AS or SC (1 μl h^{-1}, 10 nmol ml^{-1}), made in regular artificial cerebrospinal fluid (CSF) or CSF alone, using an implanted Alzet minipump (AP −0.5 mm, ML +1.0 mm from bregma, DV −2.0 mm from the skull).

Locomotor activity and CPP Test

Locomotor activity was measured using an infrared detector (Neuroscience, Tokyo, Japan) as our previous report.[18] The mice were injected with METH (1 mg kg^{-1}, s.c.) daily for 5 days (day 1–5), followed by locomotor activity measurement at days 1, 3 and 5. Conditioned place-preference (CPP) test was carried out according to the methods as described before but with modification in conditioning.[19] Briefly, a mouse was allowed to move freely between transparent and black boxes for 20 min once per day for 3 days (from day 2 to day 0) in the preconditioning. In the mornings from days 1 to 3, the mouse was treated with METH (1 mg kg^{-1}, s.c.) and put in nonpreferred box for 20 min. After an interval of 12 h the mouse was treated with saline and put in the side opposite to the METH-conditioning box for 20 min. On day 4, the post-conditioning test was performed without drug treatment, and place-conditioning behavior was expressed as post-value minus pre-value.

Microdialysis

C57BL/6 mice were anesthetized before a guide cannula was implanted in the NAc (AP +1.7 mm, ML −0.8 mm from bregma, DV −4.0 mm from the skull).[19] Meanwhile, a mini osmotic pump filled with AS, SC (10 nmol ml^{-1}) or CSF was implanted intracerebroventricularly as described above. Equal numbers of animals were assigned to METH and saline pretreatment groups. Dialysis probes were inserted to the guide cannula the night prior to the experiment. Microdialysis samples were collected every 10 min (2.0 μl min^{-1}). The DA output was presented as

relative to the baseline (the average concentration of four consecutive stable samples defined as 100%).

Western blotting and immunostaining

To determine expression of Piccolo, brain tissue or cell lysate was solubilized in homogenization buffer (150 mM NaCl, 1 mM EDTA, 10 mM Tris, 100 mM Na_2CO_3, pH 11.5) with a mixture of protease inhibitor. After shaking for 30 min and centrifugation at 4 °C, supernatants were subjected to SDS-PAGE (4% polyacrylamide) and transferred to polyvinylidene difluoride membranes. Mouse brains or cultured cells were fixed in 4% paraformaldehyde in PBS and permeabilized with 0.4% Triton X-100.

Cell culture, transfection and [³H]DA uptake

PC12 cells (Riken Bioresource Center Cell Bank, Tsukuba, Japan) were cultured on polyornithine-coated culture coverslips in Dulbecco's modified Eagle's medium (DMEM) supplemented with 10% heat-inactivated horse serum and 5% fetal bovine serum (FBS).[6] For stable expression of hDAT, PC12 cells were transfected with pCMV-hDAT using Lipofectamine 2000 (Invitrogen). A stably transfected pool was selected with 800 μg ml^{-1} geneticin (Invitrogen). For transient expression, the cells were transfected with the plasmids expressing different domain of Piccolo. The primary cultured dopaminergic neurons were separated from ventral midbrains of rat embryos (day 14). [³H]DA uptake in hDAT-PC12 cells was performed as described before.[20] Briefly, cells were washed in Krebs–Ringers–HEPES (KRH) buffer twice before assay. Uptake was initiated by adding 1 μM 3, 4-(ring-2,5,6,-³H)-DA (Perkin Elmer, Waltham, MA) containing 10^{-5} M pargyline and 10^{-5} M ascorbic acid. Uptake proceeded for 10 min at 23 °C and was terminated by three rapid washes in ice-cold KRH buffer. Accumulated [³H]DA was determined by liquid scintillation counting (Beckman LS6500). Nonspecific uptake was defined in the presence of 10 μM GBR12909 (Sigma).

Cell-surface biotinylation and internalization assays

Biotinylation internalization assays were performed as described previously.[6]

Structural models

Molecule models of Piccolo C_2A domain were generated using the amino-acid sequence data from Protein Data Bank (Gi:42543545). The C_2A domain models were energy minimized using Molecular Operating Environment (MOE) software (Chemical Computing Group, Montreal, Canada) to fix any mismatches between the various structural segments. All calculations used an MMFF94x force field and a cutoff distance of 9.5 Å for nonbinding interactions. ASEDock of the MOE program was used for phospholipids and/or Ca^{2+} ions docking stimulation. DSviewer Lite software (Accelry Inc., San Diego, USA) was used for modeling of the electrostatic surface.

Statistics

All data were expressed as means ± s.e.m. Statistical significance was determined by a one-way ANOVA, followed by the Bonferroni–Dunn test for multigroup comparisons. Differences were considered significant when $P<0.05$.

Results

Overexpression of Piccolo in the NAc of METH-treated mice

The reasons for pursuing Piccolo for intensive investigation arose from our preliminary findings in PCR-select cDNA subtraction strategy (Clontech Laboratories, Palo Alto, CA, USA) for detecting the

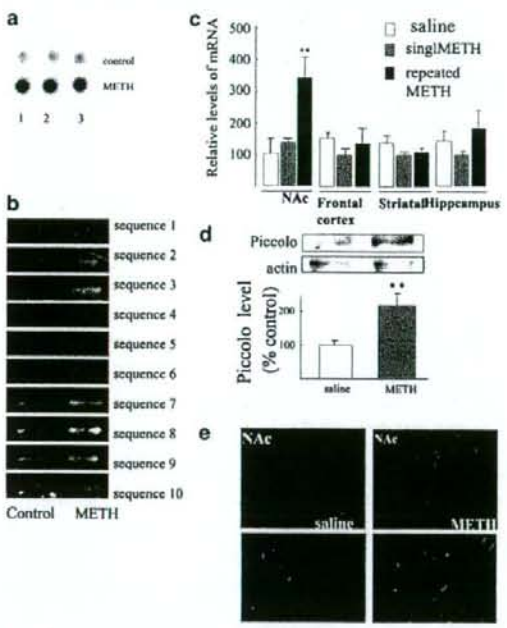

Figure 1 Piccolo expression in nucleus accumbens (NAc) was upregulated by repeated methamphetamine (METH) administration. (**a**) Piccolo overexpression in the NAc of a presentative mouse after daily METH administration for 5 days was shown. (**b**) RT–PCR analysis revealed a significant increase in the productions of the target sequences of Piccolo induced by METH. (**c**) Piccolo mRNA production was elevated significantly in NAc, rather than in the frontal cortex, striatal and hippocampus, of the mice treated with repeated METH. Data are expressed as percent of mRNA level of NAc in saline-treated mice ($n=6$). $^{**}P<0.01$, compared with saline or single dosing of METH (in NAc). (**d**) Western blotting analysis showed the elevation of Piccolo level in NAc responding to repeated METH. $^{**}P<0.01$, compared with saline. (**e**) Immunostaining showed the elevation of Piccolo immunoreactivity in the NAc of the mice administrated with repeated METH. Saline-treated mice (left column) and METH-treated mice (right column).

affected genes in the NAc by METH. The C57BL/6J mice were daily administrated with METH (2 mg kg^{-1}, s.c.) for 5 days, and Piccolo mRNA production in the NAc was found to increase by 240% in comparison to that of saline-treated mice (Figure 1a). Although little is known about the function of Piccolo in drug-induced behavioral sensitization, its subcellular localization, molecular functions and interacting partners led us to presume that Piccolo overexpression elicited by METH could be involved in DA signaling strength and presynaptic plasticity.

We performed a series of experiments to validate the results from PCR-select cDNA subtraction. After the mice were daily administrated with METH (1 mg kg^{-1}, s.c.) for 5 days, Piccolo mRNA levels in the NAc were measured semiquantitatively by RT–PCR. As Piccolo possesses several splicing domain structures, we amplified and analyzed 10 different target sequences. As shown in Figure 1b, repeated METH administration significantly elevated the mRNA productions of the target sequences of Piccolo in NAc. To confirm such alterations, the mRNA productions of Piccolo in different brain regions were measured quantitatively by real-time RT–PCR 2 h after single METH dosing (1 mg kg^{-1}, s.c.) or the final injection of daily METH administration (1 mg kg^{-1}, s.c.) for 5 days. As shown in Figure 1c, the levels of Piccolo mRNA in the frontal cortex, striatal or hippocampus were not affected by either single or repeated METH administration. Remarkably, Piccolo mRNA level in the NAc was increased following repeated METH administration ($F_{(2,15)}=5.58$; $P<0.05$), whereas it was not altered by single METH injection. We then examined Piccolo expression in the NAc using western blotting. Consistently, Piccolo protein level in NAc was elevated apparently after repeated METH administration ($t_{(1,8)}=7.35$; $P<0.01$; Figure 1d). Immunostaining also revealed a strengthened Piccolo immunoreactivity in NAc of the mice treated with repeated METH (Figure 1e). Taken together, our data suggest a selective increase of Piccolo expression in NAc of behaviorally sensitized mice induced by repeated METH dosing, rather than a global increase of the brain. Because NAc is a brain area closely associated with drug dependence, we presumed that Piccolo overexpression may be involved in dopaminergic plasticity in neural circuits, which is critical for reward.

Piccolo modulates behavioral plasticity and synaptic DA concentration in NAc

To correlate Piccolo expression with the behavioral and neurochemical phenotype to METH, we utilized an AS strategy, which has been widely used to manipulate gene expressions in the brain via intracerebroventricular infusion.[21] The designed AS, which directs against nucleotides 2452–2466, has been demonstrated to downregulate successfully the expression of Piccolo in previous studies.[17] Additionally, a SC was used as a control.

The mice were infused continuously with AS, SC or CSF using implanted osmotic minipumps for 3 days before daily saline or METH administration (1 mg kg^{-1}, s.c.) for 5 days. Such infusion was sustained till the end of each behavioral test. Locomotor activities of mice were measured at days 1, 3 and 5 immediately after drug injection (Figure 2a). There was no difference among Piccolo AS-, SC- or CSF-treated mice in baseline locomotor activity throughout a 30 min habituation period (data not shown) or in response to saline (Figure 2b). Repeated METH administration caused a progressive hyperlocomotion in mice, and interestingly, AS-pretreated mice developed a greater hyperlocomotor activity than those treated with SC or CSF after METH administration for 3 days ($F_{(2,15)}=5.47$; $P<0.05$; Figure 2c). Furthermore, such enhanced hyperlocomotor activity was sustained till day 5 despite that the difference was not significant compared with that of SC- or CSF-pretreated mice.

We then investigated the potential role of Piccolo in the rewarding effects by the CPP, a classical conditioning paradigm in which animals learn to prefer an environment associated with drug exposure. The mice were infused with AS, SC or CSF for 3 days before the training of CPP (Figure 2d). As shown in Figure 2e, the CSF-treated mice showed baseline preference for either side of the test chambers prior to METH administration, and developed the significant place conditioning after training with METH ($F_{(5,42)}=9.12$; $P<0.05$). Notably, the Piccolo AS-pretreated mice showed approximately a double degree of place conditioning compared to those treated with SC or CSF, indicating that the AS-treated mice developed an enhancement of rewarding effect to METH. The mice were killed immediately after the behavioral test to measure Piccolo protein levels in NAc. Piccolo expression in NAc responding to METH was dramatically increased, whereas AS effectively decreased its expression (Figure 2f). These results indicate that Piccolo downregulation was sufficient to confer METH-enhanced sensitization and rewarding effect, which is mediated predominantly by the dopaminergic system. No evidence of neurotoxicity in pathological histology was found outside of the mechanical disruption produced by implantation of the infusion cannula in our experimental conditions (data not shown).

We finally measured DA release in the NAc by a microdialysis technique. The mice were infused with Piccolo AS, SC or CSF for 3 days before daily METH administration (1 mg kg^{-1}, s.c.) for 3 days (Figure 2g). The basal levels of DA in NAc did not differ among CSF-, AS- or SC-treated mice (CSF, 0.58 ± 0.21 nM; AS, 0.49 ± 0.17 nM; SC, 0.60 ± 0.18 nM) before the final challenge of METH. As expected, DA levels in the NAc were markedly increased immediately after the final challenge of METH. Obviously, AS pretreatment promoted METH-induced DA release in the NAc compared with SC or CSF ($F_{(2,9)}=5.874$; $P<0.05$; Figure 2h). These data strongly supported

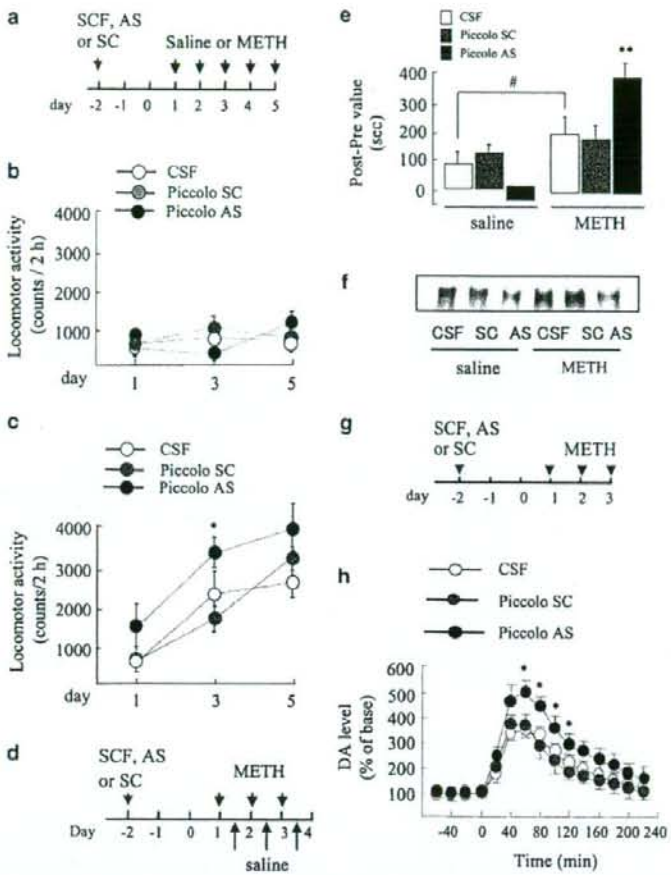

Figure 2 Downregulation of Piccolo expression with antisense oligodeoxynucleotide (AS) promoted methamphetamine (METH)-induced behavioral and synaptic plasticity. (**a–c**) Mice were infused intracerebroventricularly with Piccolo AS, scramble oligodeoxynucleotide (SC) or cerebrospinal fluid (CSF) for 3 days before daily saline (b) or METH (c) administration for 5 days. Locomotor activities were measured at days 1, 3 and 5 ($n=6$). $^{*}P<0.05$, compared with SC or CSF. (**d, e**) Mice were infused with Piccolo AS, SC or CSF for 3 days before conditioned place-preference (CPP) training. On day 4, the post-conditioning test was performed ($n=8$). $^{**}P<0.01$, compared with SC or CSF in METH-treated groups, $^{*}P<0.05$, compared with CSF in saline-treated group. (**f**) The presentative immunoblots from western blotting indicated that Piccolo expression in the nucleus accumbens (NAc) was inhibited by AS in the mice treated by repeated METH. (**g, h**) Mice were infused with AS, SC or CSF for 3 days, followed by daily METH administration for 3 days. Microdialysis was conducted after the final METH injection ($n=4$). $^{*}P<0.05$, compared with SC or CSF at the same time point.

the findings in behavioral tests, suggesting that the enhanced accumulation of DA in NAc resulted from AS may contribute to the amplified responsiveness to METH; moreover, Piccolo may play a role in modulating synaptic DA concentration. Taken these results together, Piccolo overexpression in NAc may present a mechanism of opposing the behavioral responsiveness to METH.

Piccolo is colocalized in dopaminergic neurons

To study whether Piccolo is expressed in dopaminergic neurons, double immunostaining was performed in primary cultured dopaminergic neurons. The immunoreactivities of Piccolo and TH revealed an extensive overlap along neuronal projections, indicating that Piccolo is present at dopaminergic synapse (Figure 3a). Notably, abundant Piccolo immunoreactivity was observed as clusters and puncta at the dopaminergic terminals (Figure 3b). Moreover, we also found that almost all of the DAT-immunopositive clusters were present at Piccolo-containing clusters situated along dendritic profiles (Figure 3c), implying the potential interplay of these two molecules. These results strongly support the conclusion that Piccolo is a shared component of the dopaminergic synapses.

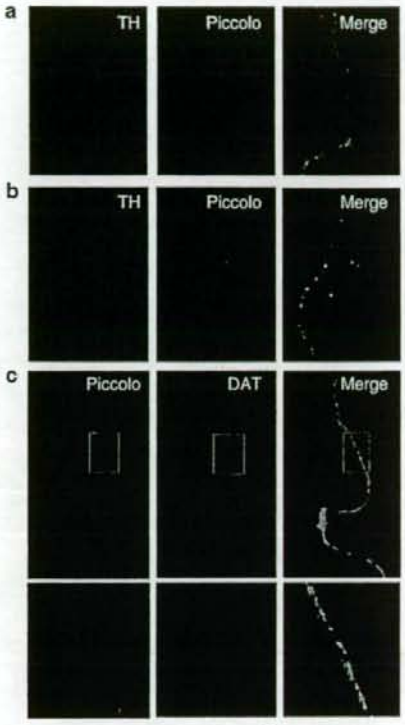

Figure 3 Expression of Piccolo in dopaminergic neurons. (a) Double immunostaining showed that Piccolo is expressed in tyrosine hydroxylase (TH)-positive neurons. (b) Abundant expression of Piccolo is present at the presynaptic component of cultured dopaminergic neurons. (c) Dopamine transporter (DAT) immunoreactivity along the dendritic profiles is paralleled with that of Piccolo.

Piccolo C_2A domain attenuates the inhibition of DA uptake induced by METH through modulating plasmalemmal DAT expression

Total DAT expression levels showed no changes when hDAT-PC12 cells were exposed to either METH (1 μM) for various time periods or concentrations for 30 min (Figures 4a and b). However, the level of cell surface hDAT was reduced in time-dependent manner, and importantly, such reduction was paralleled with the extent of the inhibition of [^{3}H]DA uptake ($F_{(4,15)} = 25.6$, $P < 0.001$; Figure 4c). Similar results were also obtained in dose-dependent studies, which showed a good correlation of the level of surface hDAT and [^{3}H]DA uptake responding to various concentrations of METH ($F_{(4,15)} = 73.0$, $P < 0.001$; Figure 4d).

The schematic representations of C_2A domain, PDZ domain and a fragment between C_2A domain and PDZ domain are shown in Figure 4e. The C_2A domain, PDZ domain or the fragment were expressed in hDAT-PC12 cells to investigate the changes in [^{3}H]DA uptake. We found that the cells transfected with C_2A domain showed a slight, but not significant, increase in [^{3}H]DA uptake in response to saline; moreover, transfection of PDZ domain or p13192 did not alter [^{3}H]DA uptake, either (Figure 4f, left panel). We then pretreated the cells with 1 μM METH for 30 min, followed by [^{3}H]DA uptake assay. METH obviously inhibited [^{3}H]DA uptake, and importantly, C_2A domain-transfected cells showed a higher level of [^{3}H]DA uptake compared with empty pCMV (Stratagene, La Jolla, CA; $F_{(3,20)} = 18.68$, $P < 0.01$), indicating that the C_2A domain expression could attenuate METH-induced inhibition of DA uptake (Figure 4f, right panel).

Because an increase in DA uptake could be resulted from more DAT molecules expressed at the cell surface, we introduced these vectors into hDAT-PC12 cells, and analyzed plasmalemmal hDAT expression by cell-surface biotinylation. The expression levels of cell-surface hDAT did not increase significantly after transfection of C_2A domain, PDZ domain or p13192 in basal conditions (Figure 4g). When the cells were pretreated with 1 μM METH for 30 min, C_2A domain transfection significantly attenuated the decrease in cell surface hDAT level compared to pCMV ($F_{(3,8)} = 14.61$, $P < 0.01$), whereas PDZ domain and p13192 showed no effects (Figure 4h). Such change was consistent with that of [^{3}H]DA uptake shown in Figure 4f, indicating that Piccolo C_2A domain may attenuate the METH-induced inhibition of DA uptake and maintain DAT expression at cell surface.

Piccolo C_2A domain modulates DAT internalization by a mechanism of membrane association

Given that DAT can be internalized and/or recycled, we speculated that the decreased lose of membrane DAT induced by METH in C_2A domain-transfected cells could be resulted from attenuated DAT internalization. To test this hypothesis, DAT internalization was measured by reversible biotinylation in hDAT-PC12 cells. We found that C_2A domain expression could not affect the basal DAT internalization, as revealed by the similar amount of internalized DAT among all groups (Figure 5a). However, DAT internalization was significantly attenuated by C_2A domain expression when the cells were exposed to 1 μM METH for 30 min ($F_{(3,8)} = 8.55$, $P < 0.01$; Figure 5b). Expression of both PDZ domain and p13192 failed to affect the basal or METH-induced DAT internalization. Double immunostaining for hDAT and c-Myc-tagged C_2A domain showed the similar findings that the cells transfected with C_2A domain still maintained a strong plasmalemmal hDAT immunoreactivity responding to METH, whereas a relatively large amount of internalized hDAT was observed in cytosolic compartments of the cells transfected with empty pCMV (Figure 5c). These results indicated that Piccolo C_2A domain attenuates METH-induced DAT internalization, which accounts for the decrease in the loss of DAT at cell surface.

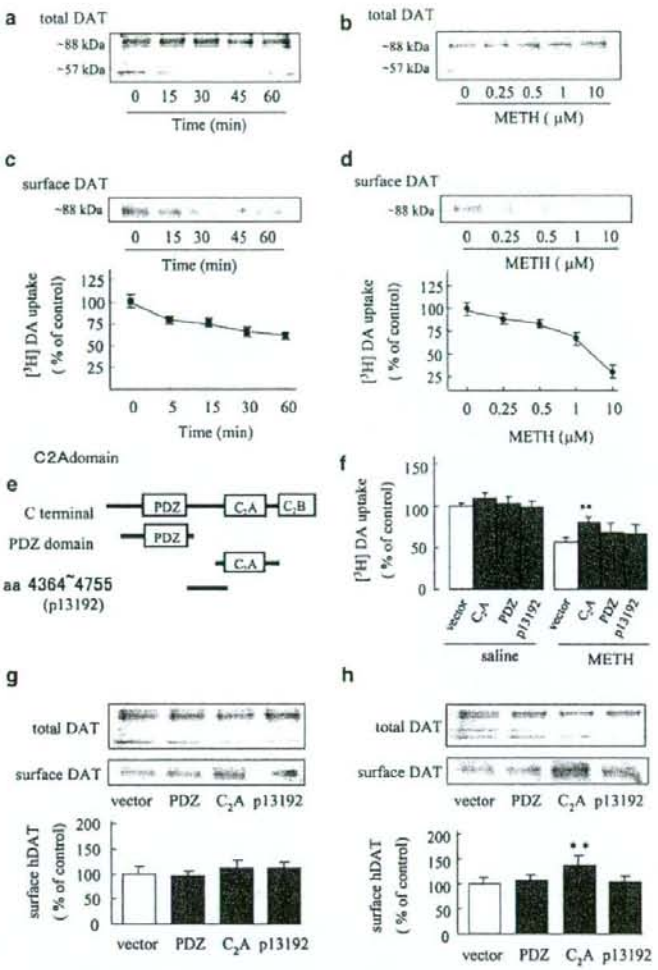

Figure 4 Piccolo C_2A domain increased dopamine (DA) uptake and dopamine transporter (DAT) surface expression. (**a**, **b**) Methamphetamine (METH) could not alter the total DAT expression levels in hDAT-PC12 cells in both time- (**a**) and dose-dependent studies (**b**). (**c**) METH (1 μM) decreased plasmalemmal DAT expression (top) in time-dependent manner, which was paralleled with the decrease in [^{3}H]DA uptake (bottom). $^{**}P<0.01$, compared with the basal level. (**d**) METH decreased DAT expression at the cell surface dose-dependently (top), which was consistent with the decrease in [^{3}H]DA uptake (bottom). $^{**}P<0.01$ and $^{*}P<0.05$, compared with the basal level. (**e**) Schematic representations of C_2A domain, PDZ domain and a fragment (amino acid 4364–4755). (**f**) Piccolo C_2A domain attenuated the METH-induced inhibition of [^{3}H]DA uptake (right panel), but failed to change the basal DA uptake (left panel) ($n=6$). $^{**}P<0.01$, compared with pCMV. (**g**, **h**) Piccolo C_2A domain could not influence DAT surface expression in hDAT-PC12 cells responding to saline (**g**). However, it attenuated METH-induced loss of surface DAT (h). $^{**}P<0.01$, compared with pCMV in METH-treated group.

To study the potential mechanism underlying the action of Piccolo C_2A domain on DAT internalization, we introduced C_2A domain into hDAT-PC12 cells and then analyzed membrane subcellular distributions of Piccolo, C_2A domain, hDAT as well as PIP_2. The cells were homogenized in regular RIPA buffer containing 1% Triton-X 100, and separated into a soluble supernatant and a particulate membrane fraction (120 000 g, 60-min pellet). The latter was solubilized again in RIPA buffer or RIPA buffer containing 0.1 M Na_2CO_3 (pH 11.5), which can extract a major part of detergent-resistant Piccolo protein from brain tissues.[12] As shown in Figure 5d, Piccolo, Piccolo C_2A domain and PIP_2 did not fractionate like a soluble cytosolic protein but was mainly found in membrane sediment extracted by Na_2CO_3, indicating that a substantial

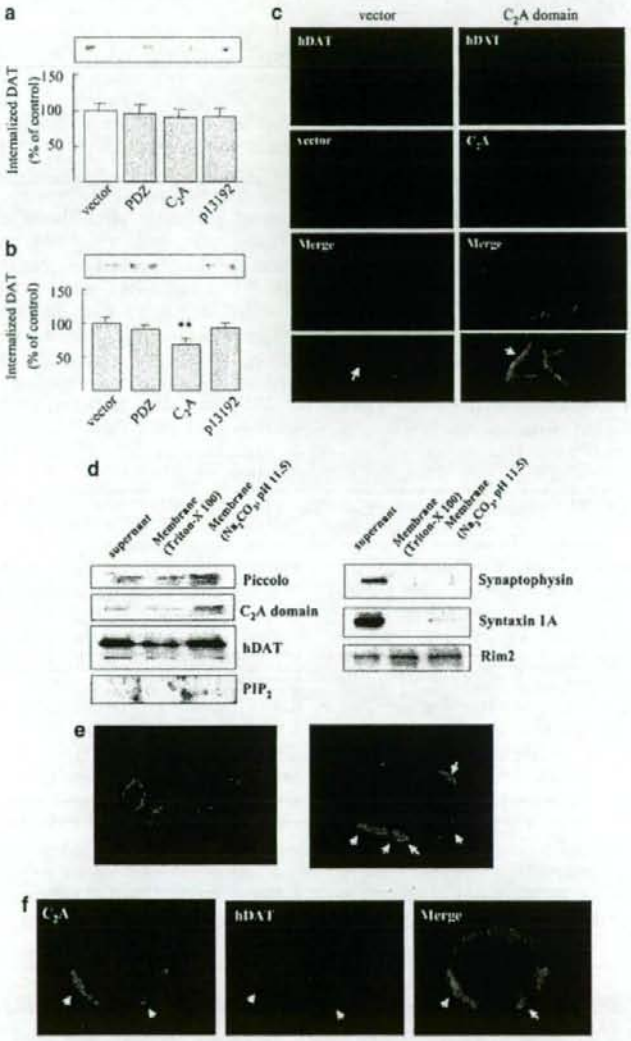

Figure 5 Piccolo modulates dopamine transporter (DAT) internalization by a mechanism of membrane association. (**a, b**) After transfection with various vectors the hDAT-PC12 cells were biotinylated and treated with either saline (**a**) or 1 μM methamphetamine (METH) (**b**) for 30 min to initiate endocytosis. Top, representative blots of internalized hDAT. Bottom, quantitation of hDAT immunoreactivity. $P<0.01$, compared with empty vector (pCMV) in METH-treated group. (**c**) The internalization of hDAT (red) was triggered by exposure of 1 μM METH for 30 min. The cells transfected with empty vector (pCMV) show enriched internalized hDAT (left panel), whereas the cells transfected with c-Myc-tagged-C_2A domain (green) reveal the strong plasmalemmal hDAT immunoreactivity (right panel). Internalized hDAT is depicted. (**d**) Distributions of Piccolo, c-Myc-tagged C_2A domain, hDAT, PIP_2 and other presynaptic proteins in hDAT-PC12 cells. The cells and membrane fractions were extracted with RIPA buffer containing 0.1 M Na_2CO_3 (pH 11.5) or not. (**e**) The transfected Piccolo C_2A domain specially targets plasma membrane in hDAT-PC12 cells. (**f**) Piccolo C_2A domain shows a paralleled immunoreactivity pattern at plasmalemmal rafts with hDAT (arrowhead).

fraction of membrane-bound Piccolo, C_2A domain and PIP_2 are associated with the same plasmalemmal rafts. Interestingly, a significant amount of hDAT was also recovered in both soluble fraction and membrane sediment extracted by Na_2CO_3, indicating that a relatively major part of membrane DAT is localized at the same subcellular fraction with Piccolo C_2A domain and PIP_2. The similar distributions of these

components in lipid raft fractions hint that C_2A domain–PIP_2 interaction may be involved in the distribution of plasmalemmal DAT. In contrast, syntaxin 1A and synaptophysin, the integral membrane proteins, were almost completely recovered in soluble cytosolic fraction, but not in a detergent-resistant fraction. Rim 2, a scaffolding protein with C_2 domain, is known to interact with Piccolo and to regulate presynaptic events. However, its similar subdistribution in the three fractions was different from that of Piccolo C_2A domain. To get an insight into the interplay among DAT, Piccolo C_2A domain and PIP_2, double immunostaining was performed. We found that Piccolo C_2A domain mainly anchored nonuniformly to the inner leaflet of plasma membrane (Figure 5e), which is consistent with its property of targeting membrane PIP_2. Notably, the distribution pattern of C_2A domain resembled that of hDAT, as revealed by the paralleled immunoreactivities at membrane microdomains (Figure 5f).

Internalization of plasmalemmal DAT is PIP_2-dependent

The concept of PIP_2 as a spatially localized regulator of membrane trafficking is clearly illustrated by its key role in clathrin-mediated endocytosis for transporter. If plasmalemmal DAT is triggered to internalize by METH, it should be accompanied by PIP_2 for recruiting endocytic adaptors through PIP_2-binding modules. To test this idea, hDAT and PIP_2 were double-stained in hDAT-PC12 cells after treatment of saline or 1 μM METH for 30 min. Surprisingly, the internalized DAT triggered by METH was found to colocalize with the PIP_2 in the cytosolic compartment (Figure 6, bottom panel), whereas the saline-treated cells only showed the constitutively internalized PIP_2 and DAT (Figure 6, top panel). These results further demonstrated that DAT internalization is also a clathrin-dependent process requiring the assembly of endocytic components like PIP_2.

Interaction of Piccolo C_2A domain and PIP_2

Although Piccolo C_2A domain binding to PIP_2 has been demonstrated using artificial membranes,[15] there is no evidence indicating interaction of the two molecules in living models. We first investigated whether plasmalemmal clusters of Piccolo immunoreactivity coincide with sites of local PIP_2 accumulation using double immunostaining. The clusters of Piccolo immunoreactivities in dendrite profile colocalized precisely with those of PIP_2 in the primary cultured dopaminergic neurons (Figure 7a). Moreover, the localization of transfected C_2A domain in hDAT-PC12 cells was similar with that of PIP_2, which revealed a patchy staining pattern at plasma membrane (Figure 7b). Importantly, the clusters with strong immunoreactivity of C_2A domain also showed substantially larger and stronger labeling macroscopic of PIP_2 clusters, indicating that C_2A domain may sequester PIP_2, thus augmenting the formation of microscopically detectable plasmalemmal PIP_2 clusters.

To better understand the interaction of the two molecules, we generated a PIs binding model of Piccolo C_2A domain with Ca^{2+} docking. As show in Figure 7c, the three-dimensional structure indicated that the predicted PIs binding sites are Ca^{2+}-binding loops at the top of C_2A domain, which shows the similar binding residues for phosphatidylinositol (PI), phosphatidylinositol 4-phosphate (PIP) and PIP_2. Notably, the crystal packing contacts for PIP_2 were the clusters of basic/aromatic residues including 4668–4670 (DNN), 4697–4698 (QK), 4738–4743 (DYDRFS) and 4746 (D). The potential importance of these residues is highlighted by the fact that they are completely conserved among rat, mouse, human and chicken Piccolo.[22] Calculation of the electrostatic surface potential of C_2A domain showed that PIP_2 binding sites are positively charged (Figure 7d), further indicating that clustering PIs by C_2A domain depends on electrostatic interactions between the

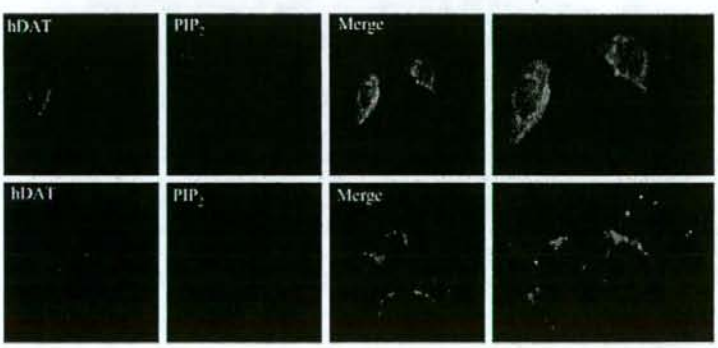

Figure 6 Piccolo C_2A domain attenuates dopamine transporter (DAT) internalization responding to methamphetamine (METH). Double-immunostaining of PIP_2 (red) and hDAT (green) in hDAT-PC12 cells. The internalization of hDAT was promoted by METH, which is accompanied by PIP_2 (bottom panel). The saline-treated cells show strong immunoreactivities of both hDAT and PIP_2 (top panel).

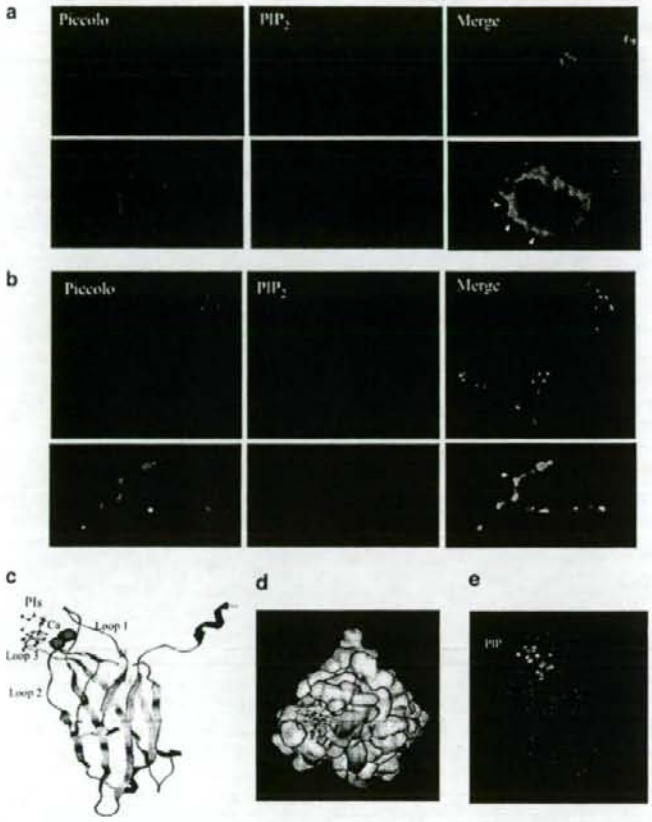

Figure 7 Interaction of Piccolo and PIP_2. (**a**) PIP_2 (red) colocalizes precisely with Piccolo (green) along the presynaptic terminal in primary cultured dopaminergic neurons (arrowed). (**b**) PIP_2 (red) accumulates at plasmalemmal rafts, where it colocalizes with Piccolo (green) in hDAT-PC12 cells. Arrowheads point to regions of intense staining of PIP_2 and Piccolo. (**c**) Model of Piccolo C_2A domain with three bound Ca^{2+} ions on top (green spheres). The top surface of C_2A domain shows the binding sites for the headgroups of PIs. (**d**) Surface plot showing the electrostatic potential of C_2A domain. Blue, positive; red, negative charge; white, neutral. PIP_2 is pointed. (**e**) Space-filling model of PIP_2 is shown on top in pink C_2A domain, which provides a cupped shape of polybasic region to accommodate PIP_2.

positively charged residues in proteins and the negatively charged headgroups of PIs. The lowest binding energies of Piccolo C_2A domain for PI, PIP and PIP_2 with Ca^{2+} docking were −59.491, −93.229 and −102.642 Kcal, respectively, suggesting a specific interaction between PIP_2 and C_2A domain. Furthermore, the space-filling model showed that PIP_2 is tightly packed against the top surface of C_2A domain, which forms a favorable pocket to accommodate the moiety of PIP_2 (Figure 7e).

Piccolo regulated DAT function not through syntaxin 1A

As syntaxin 1A has been demonstrated to regulate the expressions and activities of serotonin transporter (SERT) and γ-aminobutyric acid (GABA) transporters,[23,24] Piccolo might regulate DAT surface expression through interaction with syntaxin 1A. We first investigated whether syntaxin 1A could bind to Piccolo, though syntaxin is identified to bind to Piccolo.[25] The lysates from hDAT-PC12 cells were immunoprecipitated with anti-syntaxin 1A, followed by hDAT immunoblotting. As shown in Supplementary Figure 1a, hDAT were present in the lysate. As expected, we also detected co-immunoprecipitation of hDAT and syntaxin 1A in following immunoprecipitation with anti-hDAT (Supplementary Figure 1b). These results showed an apparent association of these two molecules, which was supported by previous reports.[26] We then investigated whether syntaxin 1A could regulate DAT activity. The hDAT-PC12 cells were pretreated with Bont/C1, a toxin that specifically cleaves syntaxin 1A, followed by

[^{3}H]DA uptake assay; moreover, Bont/B that specifically cleaves the vesicle *N*-ethylmaleimide-sensitive factor attachment receptor protein synaptobrevin was used as a control. As shown in Supplementary Figure 1c, Bont/C1 (0.5–5 nM) failed to alter the [^{3}H]DA uptake in the cells treated with saline. Although Bont/C1 slightly elevated [^{3}H]DA uptake in the cells exposed to METH compared with Bont/B, the difference was not significant. To exclude that such incapability of Bont/C1 in modulating DA uptake was a result of the low concentration or short exposure time, we treated the cells with Bont/C1 at 0.25 μM for 6 h. However, [^{3}H]DA uptake was also not altered (data not shown). Additionally, exposure of METH at the concentration ranging from 0.5–20 μM for 30 min did not alter the expression level of syntaxin 1A in hDAT-PC12 cells (data not shown). Taken together, these data suggest that DAT and syntaxin 1A may mechanically, but not functionally, interact. Given the incapability of syntaxin 1A itself in modulating DAT, it unlikely mediates the role of Piccolo in regulating DAT expression at plasma membrane.

Discussion

The contribution of dopaminergic transmission to behavioral sensitization has been well recognized. Expression of certain proteins appears to be compensatory adaptation to the excessive DA signaling, which could be biologically adaptive mechanisms contributing to addiction. Nevertheless, some proteins likely function in a reverse manner. For example, we have previously found that the expression of tissue plasminogen activator plays a positive role in morphine-induced synaptic plasticity,[19] whereas tumor necrosis factor-α expression in NAc inhibits METH-induced dependence.[18] Piccolo expression was upregulated by repeated METH administration and partial knockdown of Piccolo expression by antisense technique led to elevated synaptic DA concentration in the NAc and two major behavioral manifestations in mice: heightened hyperlocomotor activity and rewarding effect. These findings strongly show that Piccolo overexpression elicited by METH may serve as a homeostatic mechanism that prevents behavioral sensitization by maintaining the expression and activity of the plasmalemmal DAT.

The human Piccolo gene contains more than 25 exons spanning over 350 kb of genomic DNA maps to 7q11.23-q21.3, a region of chromosome 7 implicated as a linkage site for autism and Williams Syndrome.[22] Therefore, dysfunction of Piccolo may be involved in cognitive impairment and mental retardation.[27] The mechanism underlying Piccolo upregulation caused by METH remains to be elucidated. Nevertheless, inhibitory feedback to the excessive DA signaling would be a plausible candidate.

Piccolo has been reported to localize at the GABAergic and glycinergic presynaptic terminal,[10] and our findings in immunostaining demonstrated that it is also expressed at dopaminergic presynaptic terminal. DAT can be internalized from the plasma membrane at a relatively rapid rate, which provides a mechanism by which the turnover rate and density of the plasmalemmal DAT can be quickly and finely modulated.[6,8] Signaling molecules, glycosylation and DAT substrates have been shown to regulate DAT membrane trafficking. Given those findings *in vivo* behaviors tests and the properties of Piccolo, we assumed that Piccolo may play a role in modulating DA flux and DAT distribution at dopaminergic terminals. To address this issue, we investigated DA uptake and membrane DAT expression in hDAT-PC12 cells expressing different functional domain of Piccolo. METH caused DA uptake inhibition in parallel with decreased DAT surface expression, which was well consistent with those works defining the dynamically internalized DAT in hDAT-PC12 cells triggered by amphetamine. These results further support the notion that redistribution of surface DAT caused by METH-like drugs may present an important mechanism underlying the consequently reduced DAT activity. Our data showed that Piccolo C_2A, but not PDZ domain, attenuated METH-induced DA uptake inhibition by retaining DAT expression at cell surface. Because DAT can be internalized and/or recycled, we speculated that the decreased loss of membrane DAT could be resulted from attenuated DAT internalization. Such hypothesis was demonstrated by reversible biotinylation, which revealed the decreased DAT internalization in C_2A domain-transfected cells responding to METH.

It is well established that PIP_2 functions in regulating cytoskeleton, channels and transporters, and membrane trafficking at presynaptic terminal.[16,28,29] Especially, PIP_2 is essential at several stages of endocytosis for the sequential recruitment of adaptor and accessory proteins to endocytic sites.[30,31] METH rapidly causes both DAT internalization and conformational rearrangement to an intracellularly oriented transporter from which DA is released. Such process is proposed to be a drastic membrane movement and requires PIP_2 to assemble various molecules to form endocytic compartment. Significantly, we found that PIP_2 exhibits a similar distribution pattern with DAT at membrane microdomains. Furthermore, internalized DTA triggered by METH is accompanied with PIP_2 in endocytic compartments. These results indicate that PIP_2 is an important regulator in the process of DAT internalization.

A couple of scaffolding proteins such as GAP43, CAP23 and Dap160 have shown their ability to sequester membrane PIP_2, thus potentially modulating the endocytic process.[32,33] In this study we obtained several evidences further supporting the notion that Piccolo can electrostatically sequester PIP_2. Firstly, Piccolo C_2A domain may laterally bind membrane PIP_2, and augment PIP_2 clusters in hDAT-PC12 cells. In principle, the augmented clusters could represent the sequestration of phospholipids like PIP_2 at the plasma membrane.[34] Secondly, the crystal

packing contacts for PIP_2 were the clusters of basic/aromatic residues, which exhibit a universal capability of sequestering membrane PIP_2.[35] Thirdly, the space-filling model showed that Piccolo C_2A domain may pocket PIP_2 by a cupped shape of polybasic region, where the local positive potential electrostatically attracts the negatively charged PIP_2. Finally, C_2A domain shows stronger interacting potential with PIP_2 than PI or PIP. Our results are consistent with previous investigations indicating that PIs binding with Piccolo C_2A domain is largely driven by electrostatic interaction.[15]

Based on these findings, we speculated that Piccolo C_2A domain may regulate METH-triggered DAT internalization through sequestering PIP_2, and the findings in immunostaining strongly support this prediction. Piccolo C_2A domain mainly anchors nonuniformly to the inner leaflet, which is accompanied with the retention of DAT and PIP_2 at membrane microdomains; moreover, it clearly attenuated METH-triggered DAT and PIP_2 internalization in cytosol. These results show that Piccolo may sequester or 'control' locally PIP_2 by C_2A domain in membrane raft and suppress PIP_2-dependent endocytic process, thus leading to the attenuated DAT internalization.

How does the Piccolo C_2A domain–PIP_2 interaction fulfill a function in modulating DAT internalization and psychostimulant responsiveness? An explanation could be that the endocytic process for DAT internalization is inhibited directly through PIP_2 sequestration. Given the strong dependence of the endocytic machinery on PIP_2, more membrane PIP_2 is considerably mobilized for the accelerated DAT internalization triggered by METH. This situation would place the endocytic machinery of dopaminergic presynaptic terminal in a compromised position of insufficient availability of PIP_2, and thus slowing down the DAT internalization. Similarly, a dominant-negative mutant of dynamin I, a component of endocytic machinery, inhibits both PKC- and amphetamine-dependent DAT internalization;[7,36] interruption of adaptor proteins present in clathrin-coated pits like epsin interferes with DAT endocytosis.[37] Another explanation could be that Piccolo C_2A domain may retain DAT at cell surface by promoting membrane stability. METH causes both DAT internalization and conformational rearrangement to an intracellularly oriented transporter from which DA is released. In this process PIP_2 acts as a positive regulator in modulating actin filament assembly and membrane movement by creating membrane microdomains and binding proteins with lipid-specific interaction.[38,39] Therefore, overexpressed Piccolo elicited by METH may enhance the association with membrane PIP_2 or other PIs through C_2A domain and disturb PIP_2-dependent actin assembly, thereby strengthening membrane stability and weakening DAT internalization. In this case, Piccolo may function as a general stabilizer for plasma membrane and DAT. It is worth noting that protein interacting with C kinase 1 (PICK1), a skeletal component, may also stabilize and maintain DAT at plasma membrane.[40]

Piccolo likely binds to syntaxin 1A through its C_2A domain, because synaptotagmin C_2A domain which shares a great structural similarity with Piccolo C_2A domain interacts with syntaxin 1A.[15,40] Syntaxin 1A directly regulates the expressions and activities of SERT and GABA transporter.[23,24] Interestingly, a recent work has identified that syntaxin 1A also binds to DAT.[26] However, Piccolo C_2A domain appears not to regulate METH-induced DAT internalization through syntaxin 1A, because DA uptake is not affected when syntaxin 1A is inhibited.

Our findings reveal that Piccolo is capable of regulating METH-induced DAT internalization, leading to the change of DA signaling and synaptic strength. The precise mechanism underlying the role of C_2A domain–PIP_2 interplay in DAT internalization remains to be determined. No matter which mechanism could be more reasonable, sequestration of PIP_2 in lateral domains through C_2A domain appears to be important for Piccolo to regulate DAT internalization. Therefore, a greater understanding of the molecular regulators for PIP_2, which governs DAT trafficking, would shed light on the modulation of DAT surface presentation. Further investigation measuring membrane fluorescence resonance energy transfer and PIP_2 turnover/mobilization will help interpret the contribution of the proposed mechanisms.

The present investigation illustrates a paradigm that Piccolo, a presynaptic scaffolding protein, targets membrane PIP_2 by its C_2A domain, contributing to the regulation of DAT internalization. Piccolo upregulation may represent a homeostatic response of dopaminergic neurons in the NAc to excessive dopaminergic transmission, dampening hypersensitivity and rewarding effect.

Acknowledgments

We are thankful to Dr Seino Susumu and Dr Shibasaki Takao (Division of Cellular and Molecular Medicine, Kobe University Graduate School of Medicine, Japan) for the kind gifts of pCMV-HA-Piccolo-PDZ, pCMV-Myc-Piccolo-C_2A and pGEX4T-GST-p13192. We thank Mrs Nobushi Hamada and Yoshiyuki Nakamura radioisotope Center Medical Branch, Nagoya University School of Medicine for technical support. This study was supported in part by a Grant-in-Aid for Science Research and Special Coordination Funds for Promoting Science and Technology, Target-Oriented Brain Science Research Program and 21st Century Center of Excellence Program 'Integrated Molecular Medicine for Neuronal and Neoplastic Disorders' and 'Academic Frontier Project for Private Universities (2007–2011), from the Ministry of Education, Culture, Sports, Science and Technology of Japan; by a Grant-in-Aid for Health Science Research on Regulatory Science of Pharmaceuticals and Medical Devices, and Comprehensive Research on Aging and Health from the

Ministry of Health, Labor and Welfare of Japan; by a Smoking Research Foundation Grant for Biomedical Research and Takeda Science Foundation.

References

1 Kahlig KM, Binda F, Khoshbouei H, Blakely RD, McMahon DG, Javitch JA *et al*. Amphetamine induces dopamine efflux through a dopamine transporter channel. *Proc Natl Acad Sci USA* 2005; **102**: 3495–3500.
2 Sulzer D, Chen TK, Lau YY, Kristensen H, Rayport S, Ewing A. Amphetamine redistributes dopamine from synaptic vesicles to the cytosol and promotes reverse transport. *J Neurosci* 1995; **15**: 4102–4108.
3 Sandoval V, Riddle EL, Ugarte YV, Hanson GR, Fleckenstein AE. Methamphetamine-induced rapid and reversible changes in dopamine transporter function: an *in vitro* model. *J Neurosci* 2001; **21**: 1413–1419.
4 Holton KL, Loder MK, Melikian HE. Nonclassical, distinct endocytic signals dictate constitutive and PKC-regulated neurotransmitter transporter internalization. *Nat Neurosci* 2005; **8**: 881–888.
5 Sorkina T, Hoover BR, Zahniser NR, Sorkin A. Constitutive and protein kinase C-induced internalization of the dopamine transporter is mediated by a clathrin-dependent mechanism. *Traffic* 2005; **6**: 157–170.
6 Loder MK, Melikian HE. The dopamine transporter constitutively internalizes and recycles in a protein kinase C-regulated manner in stably transfected PC12 cell lines. *J Biol Chem* 2003; **278**: 22168–22174.
7 Saunders C, Ferrer JV, Shi L, Chen J, Merrill G, Lamb ME *et al*. Amphetamine-induced loss of human dopamine transporter activity: an internalization-dependent and cocaine-sensitive mechanism. *Proc Natl Acad Sci USA* 2000; **97**: 6850–6855.
8 Sorkina T, Doolen S, Galperin E, Zahniser NR, Sorkin A. Oligomerization of dopamine transporters visualized in living cells by fluorescence resonance energy transfer microscopy. *J Biol Chem* 2003; **278**: 28274–28283.
9 Zhai RG, Vardinon-Friedman H, Cases-Langhoff C, Becker B, Gundelfinger ED, Ziv NE *et al*. Assembling the presynaptic active zone: a characterization of an active one precursor vesicle. *Neuron* 2001; **29**: 131–143.
10 Fenster SD, Chung WJ, Zhai R, Cases-Langhoff C, Voss B, Garner AM *et al*. Piccolo, a presynaptic zinc finger protein structurally related to bassoon. *Neuron* 2000; **25**: 203–214.
11 Fenster SD, Kessels MM, Qualmann B, Chung WJ, Nash J, Gundelfinger ED *et al*. Interactions between Piccolo and the actin/dynamin-binding protein Abp1 link vesicle endocytosis to presynaptic active zones. *J Biol Chem* 2003; **278**: 20268–20277.
12 Wang X, Kibschull M, Laue MM, Lichte B, Petrasch-Parwez E, Kilimann MW. Aczonin, a 550-kD putative scaffolding protein of presynaptic active zones, shares homology regions with Rim and Bassoon and binds profilin. *J Cell Biol* 1999; **147**: 151–162.
13 Garner CC, Nash J, Huganir RL. PDZ domains in synapse assembly and signaling. *Trends Cell Biol* 2000; **10**: 274–280.
14 Garcia J, Gerber SH, Sugita S, Sudhof TC, Rizo J. A conformational switch in the Piccolo C2A domain regulated by alternative splicing. *Nat Struct Mol Biol* 2004; **11**: 45–53.
15 Gerber SH, Garcia J, Rizo J, Sudhof TC. An unusual C(2)-domain in the active-zone protein piccolo: implications for Ca(2+) regulation of neurotransmitter release. *EMBO J* 2001; **20**: 1605–1619.
16 Cremona O, De Camilli P. Phosphoinositides in membrane traffic at the synapse. *J Cell Sci* 2001; **114**: 1041–1052.
17 Fujimoto K, Shibasaki T, Yokoi N, Kashima Y, Matsumoto M, Sasaki T *et al*. Piccolo, a Ca^{2+} sensor in pancreatic beta-cells. Involvement of cAMP-GEFII.Rim2.Piccolo complex in cAMP-dependent exocytosis. *J Biol Chem* 2002; **277**: 50497–50502.
18 Nakajima A, Yamada K, Nagai T, Uchiyama T, Miyamoto Y, Mamiya T *et al*. Role of tumor necrosis factor-alpha in methamphetamine-induced drug dependence and neurotoxicity. *J Neurosci* 2004; **24**: 2212–2225.
19 Nagai T, Yamada K, Yoshimura M, Ishikawa K, Miyamoto Y, Hashimoto K *et al*. The tissue plasminogen activator-plasmin system participates in the rewarding effect of morphine by regulating dopamine release. *Proc Natl Acad Sci USA* 2004; **101**: 3650–3655.
20 Melikian HE, Buckley KM. Membrane trafficking regulates the activity of the human dopamine transporter. *J Neurosci* 1999; **19**: 7699–7710.
21 Bowers MS, McFarland K, Lake RW, Peterson YK, Lapish CC, Gregory ML *et al*. Activator of G protein signaling 3: a gatekeeper of cocaine sensitization and drug seeking. *Neuron* 2004; **42**: 269–281.
22 Fenster SD, Garner CC. Gene structure and genetic localization of the PCLO gene encoding the presynaptic active zone protein Piccolo. *Int J Dev Neurosci* 2002; **20**: 161–171.
23 Quick MW. Regulating the conducting states of a mammalian serotonin transporter. *Neuron* 2003; **40**: 537–549.
24 Deken SL, Beckman ML, Boos L, Quick MW. Transport rates of GABA transporters: regulation by the N-terminal domain and syntaxin 1A. *Nat Neurosci* 2002; **3**: 998–1003.
25 Shapira M, Zhai RG, Dresbach T, Bresler T, Torres VI, Gundelfinger ED *et al*. Unitary assembly of presynaptic active zones from Piccolo-Bassoon transport vesicles. *Neuron* 2003; **38**: 237–252.
26 Lee KH, Kim MY, Kim DH, Lee YS. Syntaxin 1A and receptor for activated C kinase interact with the N-terminal region of human dopamine transporter. *Neurochem Res* 2004; **29**: 1405–1409.
27 Weidenhofer J, Bowden NA, Scott RJ, Tooney PA. Altered gene expression in the amygdala in schizophrenia: up-regulation of genes located in the cytomatrix active zone. *Mol Cell Neurosci* 2006; **31**: 243–250.
28 Suh BC, Hille B. Regulation of ion channels by phosphatidylinositol 4,5-bisphosphate. *Curr Opin Neurobiol* 2005; **15**: 370–378.
29 Kanzaki M, Furukawa M, Raab W, Pessin JE. Phosphatidylinositol 4,5-bisphosphate regulates adipocyte actin dynamics and GLUT4 vesicle recycling. *J Biol Chem* 2004; **279**: 30622–30633.
30 Slepnev VI, De Camilli P. Accessory factors in clathrin-dependent synaptic vesicle endocytosis. *Nat Rev Neurosci* 2000; **1**: 161–172.
31 Itoh T, Koshiba S, Kigawa T, Kikuchi A, Yokoyama S, Takenawa T. Role of the ENTH domain in phosphatidylinositol-4,5-bisphosphate binding and endocytosis. *Science* 2001; **291**: 1047–1051.
32 Laux T, Fukami K, Thelen M, Golub T, Frey D, Caroni P. GAP43, MARCKS, and CAP23 modulate PI(4,5)P(2) at plasmalemmal rafts, and regulate cell cortex actin dynamics through a common mechanism. *J Cell Biol* 2000; **86**: 2188–2207.
33 Marie B, Sweeney ST, Poskanzer KE, Roos J, Kelly RB, Davis GW. Dap160/intersectin scaffolds the periactive zone to achieve high-fidelity endocytosis and normal synaptic growth. *Neuron* 2004; **43**: 207–219.
34 Kwik J, Boyle S, Fooksman D, Margolis L, Sheetz MP, Edidin M. Membrane cholesterol, lateral mobility, and the phosphatidylinositol 4,5-bisphosphate-dependent organization of cell actin. *Proc Natl Acad Sci USA* 2003; **100**: 13964–13969.
35 Daniels GM, Amara SG. Regulated trafficking of the human dopamine transporter-clathrin-mediated internalization and lysosomal degradation in response to phorbol esters. *J Biol Chem* 1999; **274**: 35794–35801.
36 Sorkina T, Miranda M, Dionne KR, Hoover BR, Zahniser NR, Sorkin A. RNA interference screen reveals an essential role of Nedd4-2 in dopamine transporter ubiquitination and endocytosis. *J Neurosci* 2006; **26**: 8195–8205.
37 Nebl T, Oh SW, Luna EJ. Membrane cytoskeleton: PIP(2) pulls the strings. *Curr Biol* 2000; **10**: R351–R354.
38 Gruenberg J. Lipids in endocytic membrane transport and sorting. *Curr Opin Cell Biol* 2003; **15**: 382–388.
39 Torres GE, Yao WD, Mohn AR, Quan H, Kim KM, Levey AI *et al*. Functional interaction between monoamine plasma membrane transporters and the synaptic PDZ domain-containing protein PICK1. *Neuron* 2001; **30**: 121–134.
40 Shao X, Li C, Fernandez I, Zhang X, Sudhof TC, Rizo J. Synaptotagmin-syntaxin interaction: the C2 domain as a Ca2+-dependent electrostatic switch. *Neuron* 1997; **18**: 133–142.

Supplementary Information accompanies the paper on the Molecular Psychiatry website (http://www.nature.com/mp)

Molecular Psychiatry (2008) 13, 349

www.nature.com/mp

IMAGE

Piccolo regulates dopamine transporter internalization via PIP_2

X Cen[1,2], A Nitta[1], D Ibi[1,3], Y Zhao[1], M Niwa[1], K Taguchi[1], M Hamada[1], Y Ito[3], Y Ito[4], L Wang[2] and T Nabeshima[1,5]

[1]*Department of Neuropsychopharmacology and Hospital Pharmacy, Nagoya University Graduate School of Medicine, Nagoya, Japan;* [2]*National Chengdu Center for Safety Evaluation of Drugs, West China Hospital, Sichuan University, Chengdu, China;* [3]*Department of Pharmacology, College of Pharmacy, Nihon University, Chiba, Japan;* [4]*Equipment Center for Research and Education, Nagoya University Graduate School of Medicine, Nagoya, Japan and* [5]*Department of Chemical Pharmacology, Meijo University Graduate School of Pharmaceutical Sciences, Nagoya, Japan*

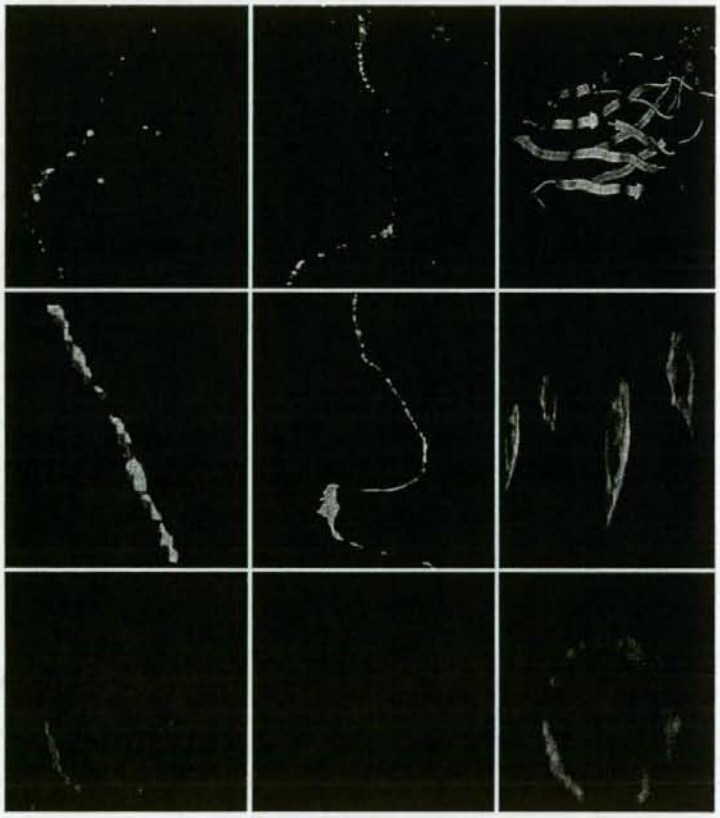

Molecular Psychiatry (2008) **13,** 349; doi:10.1038/mp.2008.17

Two left upper panels show that piccolo is not colocalized with tyrosine hydroxyls (TH)-positive neurons. Two left middle panels show that piccolo is colocalized with dopamine transporter (DAT)-positive neurons. Bottom three panels show piccolo C2A domain (left; green), dopamine transporter (middle; red) and merge image (right). Most upper right panel is docking simulation between piccolo C2A domain and PIP_2 under Ca^{2+} present condition. The right middle panel shows the piccolo C2A domain is colocalized with dopamine transporter in normal condition. For more information on this topic see the paper by Cen *et al.* on pages 451–463.

Neuropsychopharmacology (2008), 1–15

www.neuropsychopharmacology.org

Antiamnesic and Neuroprotective Effects of the Aminotetrahydrofuran Derivative ANAVEX1-41 Against Amyloid β_{25-35}-Induced Toxicity in Mice

Vanessa Villard[1,2,3], Julie Espallergues[1,2,3], Emeline Keller[1,2,3], Tursun Alkam[4,5], Atsumi Nitta[4], Kiyofumi Yamada[4], Toshitaka Nabeshima[4,6], Alexandre Vamvakides[7] and Tangui Maurice*[,1,2,3]

[1]INSERM U.710, Montpellier, France; [2]University of Montpellier 2, Montpellier, France; [3]EPHE, Paris, France; [4]Department of Neuropsychopharmacology and Hospital Pharmacy, Nagoya University Graduate School of Medicine, Nagoya, Japan; [5]Department of Basic Medicine, College of Traditional Uighur Medicine, Hotan, China; [6]Department of Chemical Pharmacology, Graduate School of Pharmaceutical Science, Meijo University, Nagoya, Japan; [7]Anavex Life Sciences, Pallini, Greece

The antiamnesic and neuroprotective activities of the new aminotetrahydrofuran derivative tetrahydro-*N*,*N*-dimethyl-5,5-diphenyl-3-furanmethanamine hydrochloride (ANAVEX1-41), a nonselective muscarinic receptor ligand and σ_1 protein activator, were examined in mice injected intracerebroventricularly with amyloid β_{25-35} ($A\beta_{25-35}$) peptide (9 nmol). $A\beta_{25-35}$ impaired significantly spontaneous alternation performance, a spatial working memory, and passive avoidance response. When ANAVEX1-41 (1–1000 μg/kg i.p.) was administered 7 days after $A\beta_{25-35}$, ie, 20 min before the behavioral tests, it significantly reversed the $A\beta_{25-35}$-induced deficits, the most active doses being in the 3–100 μg/kg range. When the compound was preadministered 20 min before $A\beta_{25-35}$, ie, 7 days before the tests, it prevented the learning impairments at 30–100 μg/kg. Morphological analysis of corticolimbic structures showed that $A\beta_{25-35}$ induced a significant cell loss in the CA1 pyramidal cell layer of the hippocampus that was prevented by ANAVEX1-41 (100 μg/kg). Increased number of glial fibrillary acidic protein immunopositive cells in the retrosplenial cortex or throughout the hippocampus revealed an $A\beta_{25-35}$-induced inflammation that was prevented by ANAVEX1-41. The drug also prevented the parameters of $A\beta_{25-35}$-induced oxidative stress measured in hippocampus extracts, ie, the increases in lipid peroxidation and protein nitration. ANAVEX1-41, however, failed to prevent $A\beta_{25-35}$-induced caspase-9 expression. The compound also blocked the $A\beta_{25-35}$-induced caspase-3 expression, a marker of apoptosis. Both the muscarinic antagonist scopolamine and the σ_1 protein inactivator BD1047 prevented the beneficial effects of ANAVEX1-41 (30 or 100 μg/kg) against $A\beta_{25-35}$-induced learning impairments, suggesting that muscarinic and σ_1 targets are involved in the drug effect. A synergic effect could indeed account for the very low active doses measured *in vivo*. These data outline the therapeutic potential of ANAVEX1-41 as a neuroprotective agent in Alzheimer's disease.
Neuropsychopharmacology advance online publication, 3 December 2008; doi:10.1038/npp.2008.212

Keywords: amyloid toxicity; σ_1 protein ligand; muscarinic ligand; oxidative stress; learning and memory

INTRODUCTION

Alzheimer disease (AD) is an irreversible, progressive and degenerative disorder damaging the higher structures of the brain (Selkoe, 1989, 2004). It is actually incurable, as the available treatments, acetylcholinesterase inhibitors or a *N*-methyl-D-aspartate receptor antagonist with neuroprotective potential, memantine, are mainly symptomatic. The pathological cleavage of amyloid precursor protein (APP) is responsible for the accumulation of amyloid-β ($A\beta$) proteins, aggregating into fibrillar oligomers and generating amyloid deposits that, in turn, form the senile plaques (Selkoe, 1989, 2004). Oligomers of $A\beta$ peptides are considered as the main factor mediating the devastating neurotoxicity observed in AD. $A\beta$ peptides vary in length from 40 to 43 amino acids, $A\beta_{1-42}$ occurring more frequently and forms fibrillar aggregates far more readily than $A\beta_{1-40}$ or $A\beta_{1-43}$ (Selkoe, 1989). Minor fragments were also identified including the highly toxic $A\beta_{25-35}$ peptide (Kubo *et al*, 2002; Gruden *et al*, 2007). The $A\beta$-mediated toxicity follows a very complex pattern. $A\beta$ oligomers form Ca^{2+} permeable pores on plasma membranes and interact with intracellular organelles regulating calcium homeostasis, the endoplasmic reticulum (ER) and mitochondria (Abramov *et al*, 2004), provoking a massive oxidative stress

*Correspondence: Dr T Maurice, INSERM U.710, EPHE, University of Montpellier II, c.c. 105, place Eugène Bataillon, 34095 Montpellier cedex 5, France, Tel: + 33 4 67 14 36 23, Fax: + 33 4 67 14 33 86, E-mail: Tangui.Maurice@univ-montp2.fr
Received 25 July 2008; revised 21 October 2008; accepted 22 October 2008